[redacted]

DECLASSIFIED

BNWL-605

C-93a Advanced Concepts
for Future Application-
Reactor Experiments

COMPARISON OF $U^{235}O_2$, $U^{233}O_2$ AND $Pu^{239}N$ FUELED CORES FOR FAST COMPACT REACTORS

By

R. M. Hiatt

Engineering Analysis Section
Engineering Development Department

BEST AVAILABLE
REPRODUCED COPY

January 1968

[redacted]

This document contains restricted data as defined in the Atomic Energy Act of 1954. Transmittal or the disclosure of its contents in any manner to an unauthorized person is prohibited.

PACIFIC NORTHWEST LABORATORY
RICHLAND, WASHINGTON

~~GROUP 1~~

[redacted]

DECLASSIFIED

Printed in USA. Available from Clearinghouse for Federal Scientific and Technical Information, National Bureau of Standards, U.S. Department of Commerce, Springfield, Virginia 22151. Price: Printed Copy $3.00; Microfiche $0.65.

COMPARISON OF $U^{235}O_2$, $U^{233}O_2$ AND $Pu^{239}N$ FUELED CORES FOR FAST COMPACT REACTORS

By

R. M. Hiatt

ABSTRACT

A comparison of $U^{233}O_2$, $U^{235}O_2$, and $Pu^{239}N$ molybdenum cermet fuelings in lithium cooled fast compact reactors operating at comparable fuel temperatures, coolant pumping powers, and reactor power levels is presented. A 10 MW_t reactor power level served as the basis for the study and graphical representation of the results effecting reactor core size, volume, and weight are shown for two models. The first model consisted of coolant tubes arranged in a triangular lattice and imbedded in a fuel matrix, and the second, contained fueled rods arranged in a triangular array. A computer code INCOMP, a steady state heat transfer code written in Fortran IV for the IBM 7090, was used to generate data for the analysis.

TABLE OF CONTENTS

LIST OF FIGURES

LIST OF TABLES

COMPARISON OF $U^{235}O_2$, $U^{233}O_2$ AND $Pu^{239}N$ FUELED CORES FOR FAST COMPACT REACTORS

R. M. Hiatt

1.0 INTRODUCTION

Because of the importance of savings in size and weight of nuclear power systems for space missions, there has been some interest in using U^{233} or plutonium as the fissile material in fast reactors for this application. Although either of these fuels will make possible a fast reactor design with lower critical mass than a U^{235} fueled reactor, the total savings in size and weight will be mitigated by other design considerations, chiefly heat removal or fuel endurance. A previous study[1] compared core design for a gas-cooled fast reactor based on nuclear, thermal, and aerodynamic considerations. The reactor used as a basis for the study was the GE-NMPO 710 Reactor. The study reported here extends the investigation to liquid metal-cooled reactors with two fuel geometries. The work was performed during 1966.

2.0 SCOPE OF STUDY

A 10 MW_t fast compact reactor cooled with lithium and fueled with 50 vol% UO_2-molybdenum cermet was used as the model. Although the study is a comparison of U^{233} and U^{235} fuels, data on plutonium fueled cores are also presented.

Identification of critical cores is determined for two fuel geometries, pins and internally-cooled hexagons, and comparison is made between the fuels and geometries at conditions of three maximum fuel temperatures and several coolant pumping powers. The data for the study were obtained from "INCOMP", a computer code written primarily for liquid coolants. Study objectives were:

- Compare the effect of fissile material choice on size and weight of critical liquid metal-cooled cores.
- Compare two core geometries, internally-cooled and fuel pin models.
- To identify useful cores sufficiently so that a subsequent comparison of transient behavior of U^{233}, U^{235} fueled reactors may be accomplished.

The following core characteristics were selected as representative of advanced high temperature liquid metal-cooled reactors and hence appropriate to this study.

TABLE 2.0-1

CORE CHARACTERISTICS FOR STUDY DESIGN POINTS

k_{eff}	1.0
Power	10 MW_t
Coolant	Lithium
Inlet Temperature	927 °C (1700 °F)
Exit Temperature	1093 °C (2000 °F)
Total Pressure Ratio*	1.0 to .75

TABLE 2.0-1 (contd.)

Fuel	50 vol% UO_2-Mo CERMET
Average Maximum Fuel Temperature	1149-1649 °C (2100-3000 °F)

* Total pressure ratio is defined as the exit coolant stagnation pressure divided by the inlet stagnation pressure.

The 10 MW_t reactor size was selected since it is large enough that the reactor size is significantly affected by thermal and hydraulic design factors. The fuel material and designs were chosen only on these bases, and not on consideration of fuel endurance. It is recognized that in a reactor of this size, the fuel element composition and design required for satisfactory endurance can have an important effect on the relative size of the cores considered in this study. However, since fuel performance under irradiation is not well characterized, these were therefore considered beyond the scope of this study. When adequate data on fuel performance become available, they should be incorporated into a reassessment of these results.

2.1 DESCRIPTION OF THE MODELS

A general description of internally-cooled cores is given in a previous report[1]. The following definitions are made for convenience and to differentiate between the two core geometries used in this study.

The fuel pin model consists of a hexagonal core arrangement with hexagonal subassemblies containing fuel pins in equilateral triangular array and with pin spacing maintained by wire-wrapping about each pin as shown in Figures C-1.1 and C-1.3.* The flats dimension in this model is considered to be approximately twice the size of its equivalent component (fuel element) in the internally-cooled core.

The internally-cooled core has the same general description as the fuel pin model. It consists of a hexagonal core arrangement containing hexagonal subassemblies defined as fuel elements. The fuel elements contain coolant tubes in equilateral triangular array embedded in a fuel matrix thus differing from the fuel pin subassembly. Figures C-1.1 and C-1.2* show typical internally-cooled cores.

2.2 BASIS OF COMPARISON

Core design parameters forming a base for fuel comparison were maximum fuel temperature, coolant pumping power, and reactor power. These parameters describe reactor performance requirements or limits sufficiently to determine core diameter, volume, and weight for the purpose of this study.

---

* See Appendix C

2.3 STUDY METHOD

Data for a comparative study of internally-cooled U^{235}, U^{233}, and Pu^{239} fuels in a fast compact gas-cooled reactor were calculated[1] using a computer code, "SWISSCHEESE"[2], written primarily for a hydraulic and heat transfer analysis of gas-cooled reactors. SWISS-CHEESE was modified to facilitate liquid coolants and used in this study. This modified version, called INCOMP, was used to calculate data based on an axial power profile and critical core sizes previously defined.[1]

Interpretation of data obtained from INCOMP was made by plotting the various parameters of interest versus a common parameter, (1-cermet fraction).* This made possible a cross-reference index relating the parameters.

2.4 ASSUMPTIONS

For expediency, it was desired to use the results of the nuclear calculations previously made for the gas-cooled reactor study if these would not introduce serious error into the comparative results. Since the previous nuclear calculations were based on tungsten diluent fuels in internally gas-cooled cores, several assumptions were necessary to

---

* (cermet fraction) is defined to be the volumetric core fraction containing 100% theoretical dense fuel.

use the critical core sizes obtained in that study. Selection of molybdenum over tungsten as the fuel diluent, because of its lower density, is considered to have a negligible effect on the nuclear conditions in the core. However, substitution of lithium for the gas coolant and conversion of the internally-cooled fuel geometries to an equivalent fuel pin model made it necessary to check the assumption that there would be no serious effect on core criticality. Table 2.4-1 shows the variation in k_{eff} obtained for three 50 vol% tungsten cermets in a previously defined internally gas-cooled core compared to k_{eff} (adjusted to 1.0) for a similar pin model fueled with a 50 vol% molybdenum cermet which was lithium cooled. A fundamental mode code, FCC[3], developed at BNW was used to generate the data. The results show the change in k_{eff} to be slightly greater for the U^{235} fueled core with values of 1.0 to 0.967 being indicated for the two models. This represents a 10% error in critical mass but was considered to be an acceptable upper limit of error for the purpose of this study commensurate with the graphical presentation of the results.

Values of 1.0 to 0.991, and 1.0 to 0.995 were experienced for U^{233} and Pu^{239} fueled cores respectively and represent only a 1% error in critical mass. Since the variations are within the accuracy of the graphs and have little effect on critical core sizing, the hydraulic and thermal analyses are considered to be appropriate for the two core geometries and complete nuclear sizing calculations were not redone for this study.

TABLE 2.4-1

VARIATION IN k_{eff} OF INTERNALLY GAS-COOLED CORES FUELED WITH TUNGSTEN CERMETS COMPARED TO LITHIUM-COOLED FUEL PIN CRITICAL CORES FUELED WITH MOLYBDENUM CERMETS AT SIMILAR CORE VOLUME FRACTIONS OF CERMET, CLADDING, AND COOLANT, AND AT AN EQUAL CORE VOLUME

Lithium-Cooled Fuel Pin Cores at 2100 °F					Equivalent Internally Gas-Cooled Cores				
Material	Core Volume Ft^3	Core Diameter Ft	Weight Grams	k_{eff}	Material	Core Volume Ft^3	Core Diameter Ft	Weight Grams	k_{eff}
	2.17	1.40		1.0		2.17	1.40		.967
Columbium			73341.84						
U^{235}			207440.67		U^{235}			207440.67	
O_2			28250.00		O_2			28250.00	
Lithium			2394.61						
Molybdenum			219389.00		Tungsten			579198.62	
	.91	1.05		1.0		.91	1.05		.991
Columbium			39395.51						
U^{233}			72982.44		U^{233}			72982.44	
O_2			10023.84		O_2			10023.84	
Lithium			1766.08						
Molybdenum			77266.13		Tungsten			234282.37	
	.60	.93		1.0		.60	.93		.995
Columbium			33316.30						
Pu^{239}			64064.00		Pu^{239}			64064.00	
N			3752.60		N			3752.60	
Lithium			1293.80						
Molybdenum			48581.30		Tungsten				

Another necessary assumption resulted from the method used to analytically define the subelements in the two core geometries. The internally-cooled core maintained a constant value of 1.5 inches for the flats dimension, thus allowing the number of fuel elements to vary with changes in (1-cermet fraction). However, subassemblies in the pin core can be larger, approximately twice the size of its equivalent fuel element in the internally-cooled core, and thus there is a decrease in the space area requirement for thermal expansion between the subelements. The selection of a constant number of subassemblies was considered to best represent the pin model and the flats dimension was allowed to vary. The assumption was made that this would not appreciably change the value of (1-cermet fraction) which is an important parameter relating the two fuel geometries and that a comparable basis for core comparison between the two models is maintained.

Since the axial power distribution curve previously reported[1] was available and shows its maximum power peaking to occur downstream from the core center, it was used in this study with the assumption that its use would cause only slightly higher maximum fuel temperatures and that the effect on core size and weight considerations would be negligible. The following core geometries and conditions (Table 2.4-2) were selected as being reasonable model representations.

TABLE 2.4-2

COMPARISON OF CORE PARAMETERS USED AS A BASIS FOR INVESTIGATING INTERNALLY-COOLED AND FUEL PIN CORE GEOMETRIES IN A FAST COMPACT LITHIUM-COOLED REACTOR

	Internally-Cooled	Pin Model
Flats Dimension	1.5 inches	Varied
Number Fuel Elements of Subassemblies	Varied	19
Fueling	50 vol% fissile compound	50 vol% fissile compound
Cermet Density (% of Theoretical)	95	95
Coolant Tube Wall Thickness (in.)	15 mils	
Fuel Rod Clad Thickness (in.)		15 mils
Subelement Spacing	4% Flats Dimension	4% Flats Dimension
Pin Spacing Maintenance by		Wire Spacers
Length/Diameter Ratio	1	1
Coolant Inlet Pressure Drop	1.5 inlet velocity heads	1.5 inlet velocity heads
Coolant Exit Pressure Drop	1.0 exit velocity heads	1.0 exit velocity heads

The high specific heat, low vapor pressure, and light weight of lithium make its usage, as a reactor coolant, most desirable. The dependence of heat removal from the fuels considered in this study was found to be a weak function of the convective film coefficient and therefore a constant value of 30,000 Btu/hr/ft $^{\circ}$F[4] was selected as appropriate. The values

of the friction factors used were those found in the literature for smooth pipes[5]. The additional pressure drop attributed to the wire wrap spacers in the fuel pin geometry was calculated according to experimental results reported in HW-65173 Rev[6].

3.0 RESULTS

3.1 SUMMARY OF MAJOR RESULTS

3.1.1 Critical Core Parameters

Critical core parameters considered to be of major importance are diameter, volume, weight, and the quantity of fissile matter present. A basis for interpretation is formed by plotting these parameters vs. (1-cermet fraction) for the three fuels. Figures I-1 through I-3 and P-1 through P-3* show these results for the two models at maximum fuel temperatures of 2100, 2500, and 3000 °F. Plotted on these curves are lines of constant pressure ratio and exit velocity. Conditions for criticality are assumed with no consideration for endurance limits.

3.1.2 Fueling Comparison

A general observation of Figures I-1 through I-3, and P-1 through P-3, shows that as the maximum fuel temperatures

---

* ((I) refers to internally cooled cores and (P) the fuel pin models in all P and I figures.)

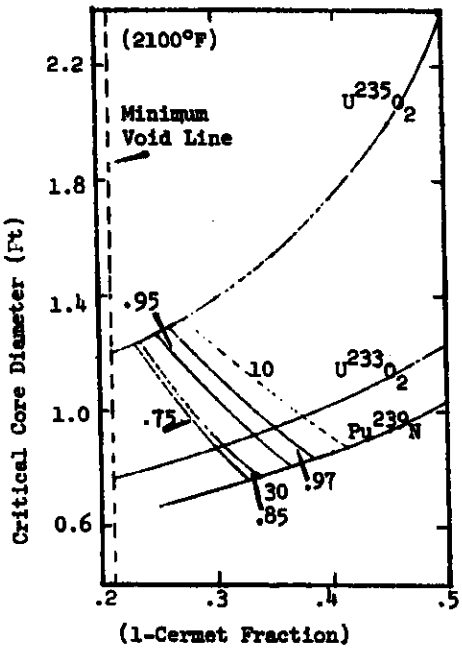

Critical Core Diameter versus (1-Cermet Fraction)

For Three Fuels, $U^{235}O_2$, $U^{233}O_2$, and $Pu^{239}N$ Embedded in a 50-50 vol. % Molybdenum Matrix. Maximum Fuel Temperatures are:
2100°F - 1149°C
2500°F - 1371°C
3000°F - 1649°C

- - - - - Lines of constant Exit Velocity; Values Indicated ft/sec.

——— Lines of constant pressure ratios, values indicated.

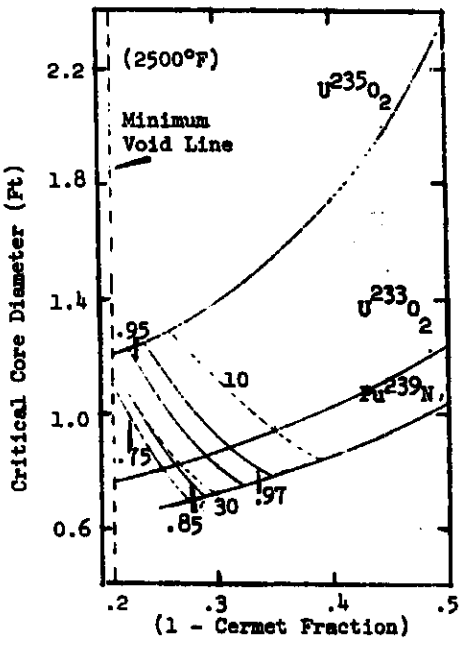

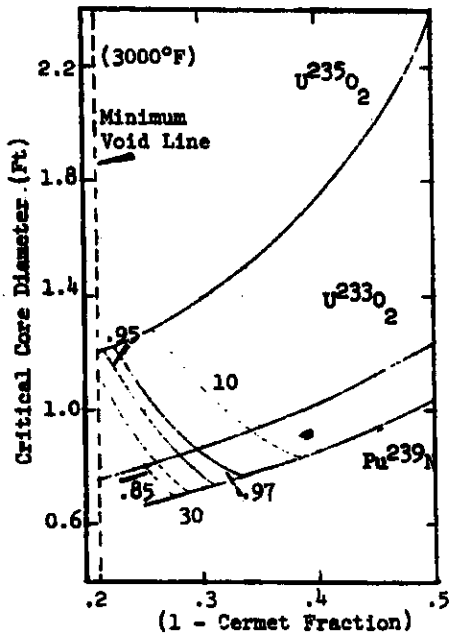

FIGURE I-1 Effect of (1 - cermet fraction) on Critical Core Diameter for Internally Cooled Cores

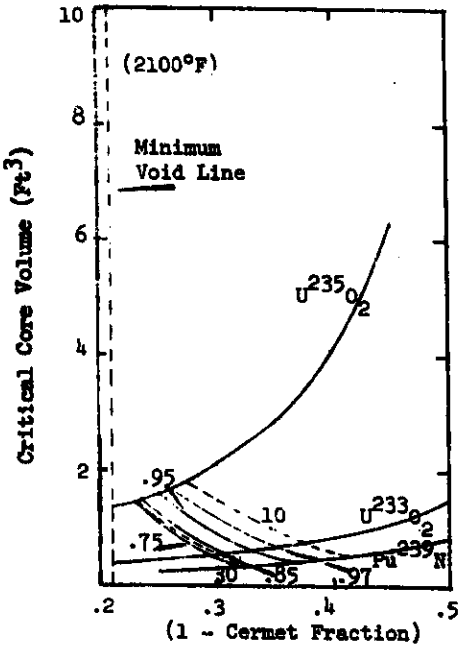

Critical Core Volume
versus
(1 - Cermet Fraction)

For Three Fuels, $U^{235}O_2$, $U^{233}O_2$, $Pu^{239}N$ Embedded in a 50-50 Vol% Molybdenum Matrix. Fuel Temperatures are:

2100°F - 1149°C
2500°F - 1371°C
3000°F - 1649°C

- - - - - - Lines of constant exit velocity; values indicated ft/sec.

——— Lines of constant pressure ratios, values indicated.

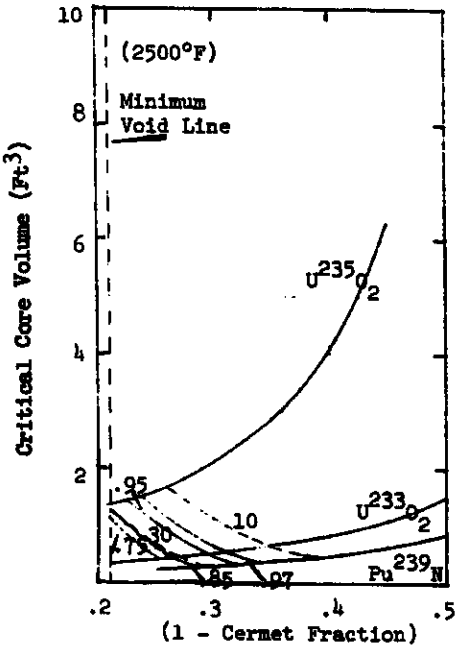

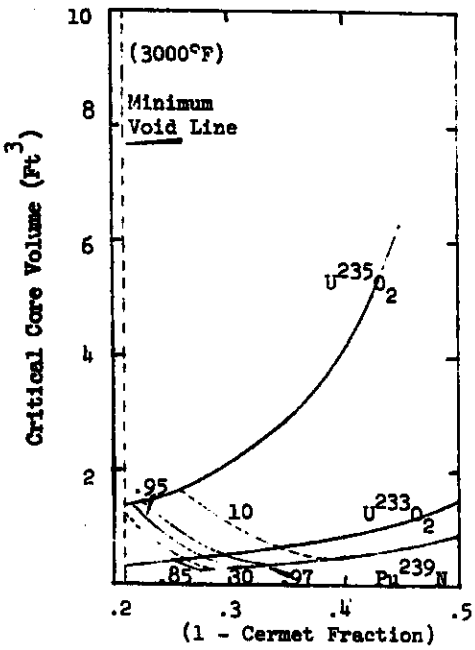

FIGURE I-2 Effect of (1-cermet fraction) on Critical Core Volume for Internally Cooled Core

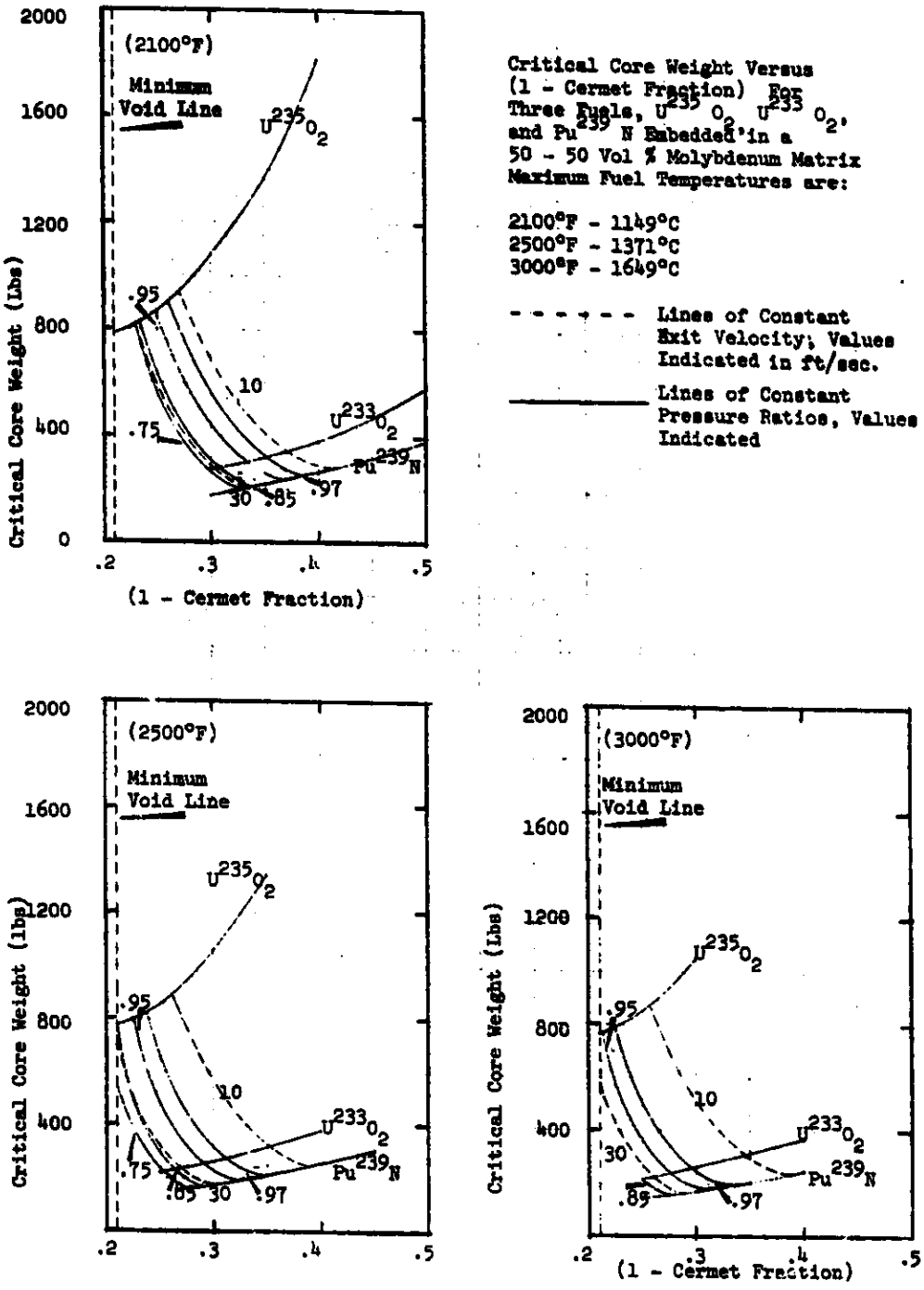

FIGURE I-3 Effect of (1 - cermet fraction) on Critical Core Weight for Internally Cooled Cores

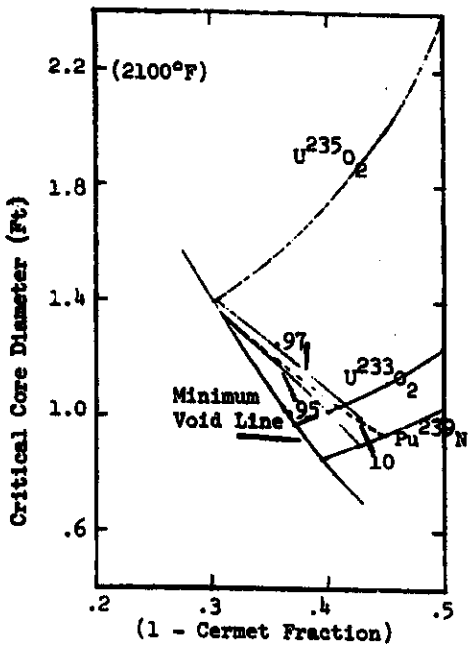

Critical Core Diameter Versus (1 - Cermet Fraction) for Three Fuels, $U^{233}O_2$, $U^{235}O_2$, and $Pu^{239}N$ Embedded in a 50-50 V/o Molybdenum Matrix. Maximum Fuel Temperatures are: 2100°F=1149°C, 2500°F=1371°C, 3000°F=1649°C

- - - - - - - Lines of Constant Exit Velocity; Values Indicated in ft/sec.

——— Lines of Constant Pressure Ratio, Values Indicated

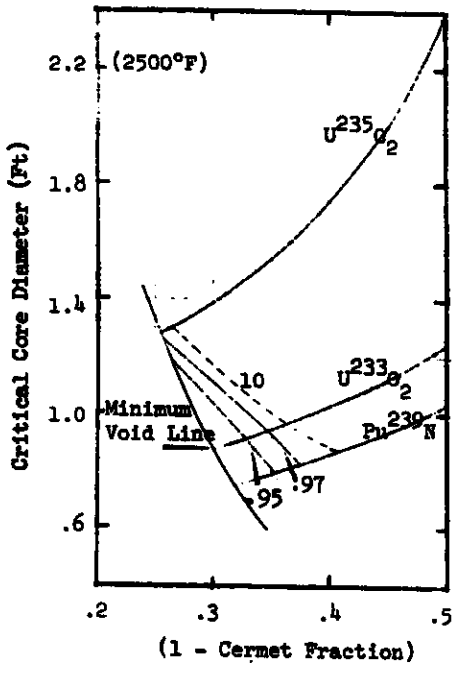

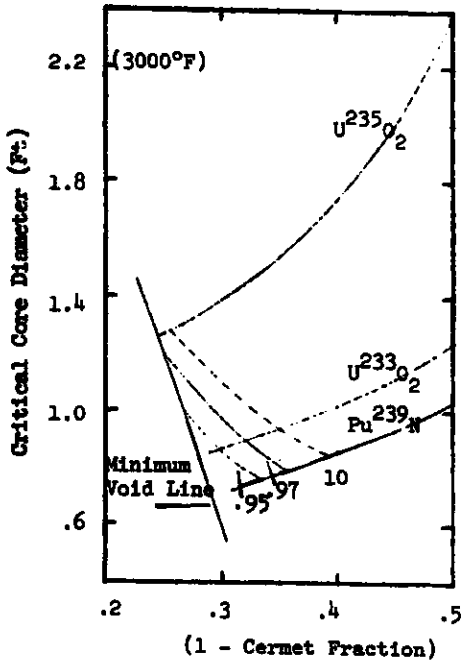

FIGURE P-1 Effect of (1 - cermet fraction) on Core Diameter for Pin Cores

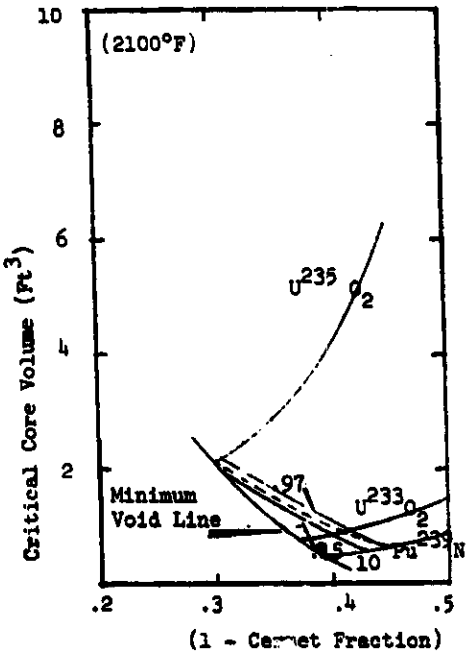

Critical Core Volume Versus (1 - Cermet Fraction) for Three Fuels, $U^{235}O_2$ $U^{233}O_2$, and $Pu^{239}N$ Embedded in a 50 - 50 Vol % Molybdenum Matrix. Maximum Fuel Temperatures are:

2100°F = 1149°C
2500°F = 1371°C
3000°F = 1649°C

- - - - - - Lines of Constant Exit Velocity, Values Indicated in Ft/Sec.

——— Lines of Constant Pressure Ratio, Values Indicated

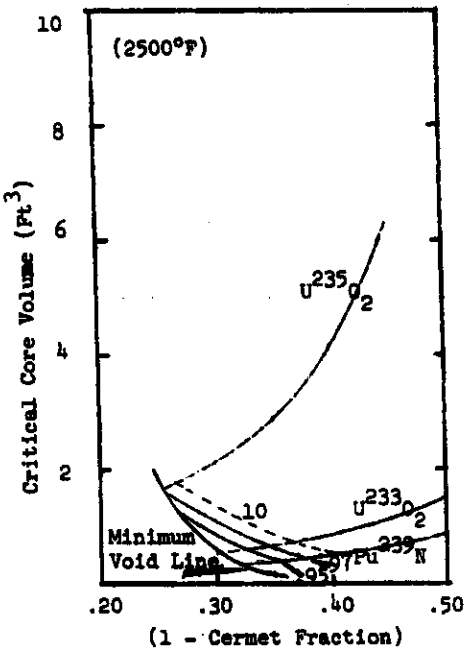

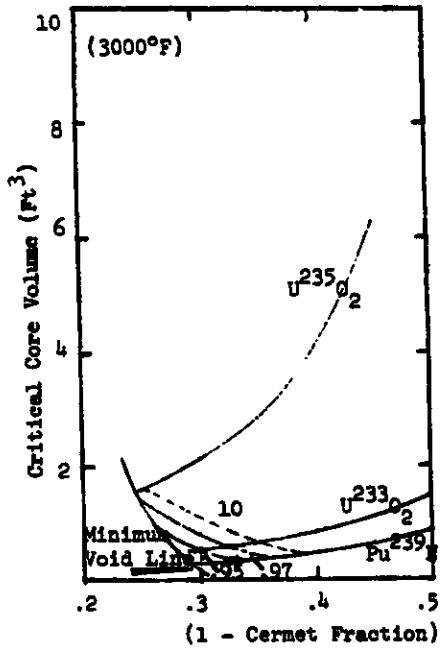

FIGURE P-2 Effect of (1 - cermet fraction) on Core Volume for Pin Cores

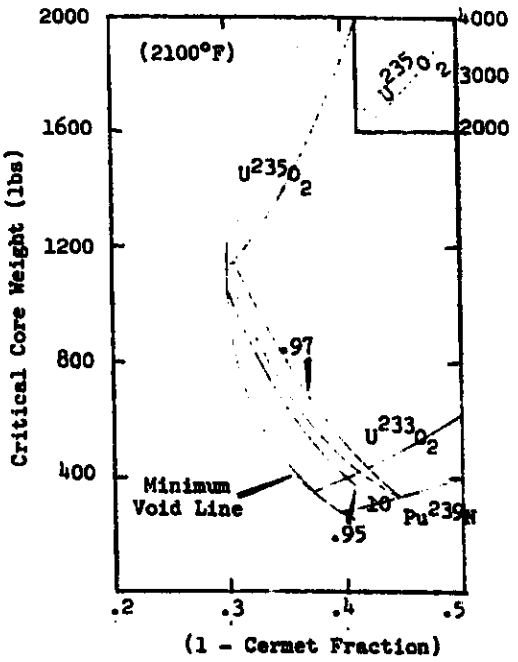

Core-Weight Versus (1 - Cermet Fraction) for Three Fuels, $U^{233}O_2$, $U^{235}O_2$, and $Pu^{239}N$ Embedded in 50 - 50 Vol % Molybdenum Matrix. Maximum Fuel Temperatures are:

2100°F = 1149°C
2500°F = 1371°C
3000°F = 1649°C

- - - - - - Lines of Constant Exit Velocity, Values Indicated in ft/sec.

——— Lines of Constant Pressure Ratio, Values Indicated

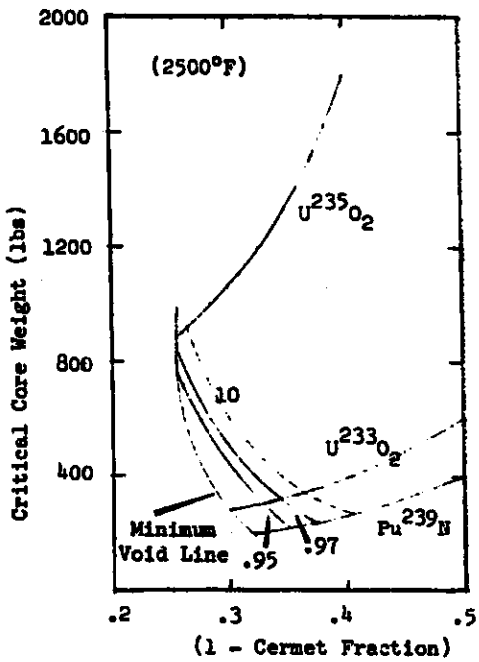

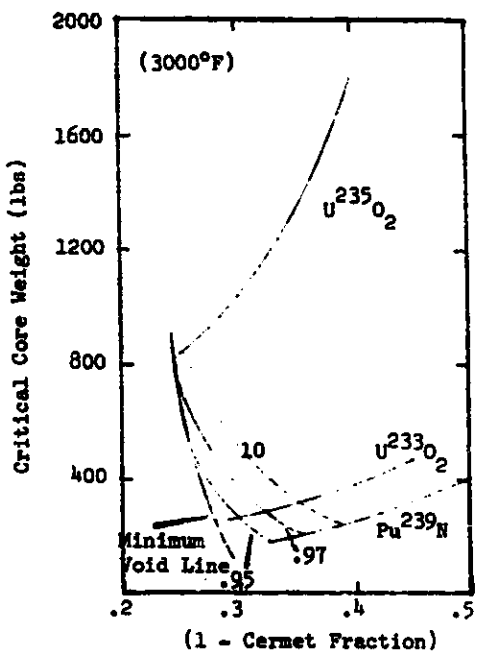

FIGURE P-3 Effect of (1 - cermet fraction) on Core Weight for Pin Cores

increase (1-cermet fraction) decreases with a consequent reduction in core diameter, volume, and weight, for any given fuel. The U^{235} fueled core shows greater change with temperature variations than the alternate more fissile material, as indicated by the slope of the lines.

Tables 3.1-1 and 3.1-2 summarize comparisons between these fuels at a common pumping power of 650 watts corresponding to a .97 total pressure ratio (3 psi pressure drop) and several fuel temperatures.

TABLE 3.1-1

REDUCTION IN CRITICAL CORE DIAMETER, VOLUME, AND WEIGHT SUPPORTED BY U^{233} AND Pu^{239} FUELS OPERATING AT 2100° F MAXIMUM FUEL TEMPERATURES L/D = 1

	% of U^{235} Cores					
	Critical Core Diameter		Critical Core Volume		Critical Core Weight	
	Internally Cooled	Fuel Pin	Internally Cooled	Fuel Pin	Internally Cooled	Fuel Pin
U^{233}	73.3	75.0	38.7	41.9	35.6	37.9
$Pu^{239}N$	65.1	66.4	26.8	27.6	27.8	28.4

It is evident from Figures I-1 through I-3 and P-1 through P-3 and from Tables 3.1-1 and 3.1-2 that the more fissile fuels markedly reduce critical core diameters, volume, and weight compared to U^{235} fueled cores. This savings is not at the expense

TABLE 3.1-2

CRITICAL CORE DIAMETER, VOLUME, WEIGHT, FISSILE MATTER, AND VOID PRESENT IN U^{235}, U^{233} and Pu^{239} 5C-50 MOLYBDENUM CERMET FUELINGS L/D = 1

		Total Pressure Ratio .97									
		Critical Core Diameter Ft		Critical Core Volume Ft^3		Critical Core Weight Lbs		Fissile Matter Lbs		(1 - cermet fraction) %	
Fuel	Temp. °F	Internally Cooled	Fuel Pin	Internally Cooled	Fuel Pin	Internally Cooled	Fuel Pin	Internally Cooled	Fuel Pin	Internally Cooled	Fuel Pin
U^{235}	2100	1.29	1.40	1.68	2.17	900	1160	375.27	453.32	25.9	30.7
U^{233}	2100	.945	1.05	.65	.91	320	440	127.2	159.5	35.0	41.8
Pu^{239}	2100	.84	.93	.45	.60	250	330	116.5	140.0	38.4	44.5
U^{235}	2500	1.25		1.5		825		344.09		23.9	
U^{233}	2500	.881	.94	.54	.65	270	320	112.2	128.2	31.0	34.5
Pu^{239}	2500	.78	.825	.37	.42	210	240	78.4	84.9	34.5	37.5
U^{235}	3000	1.22		1.45		790		338.73		22.5	
U^{233}	3000	.86	.90	.51	.60	260	280	108.1	122.9	29.6	32.0
Pu^{239}	3000	.765	.80	.35	.40	200	210	75.3	83.5	33.5	35.5

of additional pumping power or fuel temperatures since comparison is made at similar values for all the fuels. Additionally, operation at higher maximum fuel temperatures reduce critical core size and weight.

Values for U^{235} fuel pin cores do not appear at temperatures of 2500 and 3000 °F for the pumping power selected since the core volume required for U^{235} criticality is not heat transfer limited. Total pressure ratios of 0.98 (2 psi pressure drop) and 0.99 facilitate maximum fuel temperatures of 2500 °F and 3000 °F, respectively, for a 50-50 vol% $U^{235}O_2$-Mo core, but the change in core size would be small. This means that an optimum value in core size has been attained in which the removal of heat from the core is no longer a restricting influence. This may be an important consideration in evaluating endurance limits for the three fuels.

3.1.3 Comparison of Models

Figures I-1 through I-3 with P-1 through P-3 indicate that to maintain similar critical core size and weight necessitates maximum fuel temperature increases for the pin model. Observe from Table 3.1-2 that internally-cooled cores operating at fuel temperatures of 2500 °F and fueled with 50-50 vol% $Pu^{239}N$-Mo cermet weigh 210 lb while pin models must operate at maximum fuel temperatures of 3000 °F for the same weight. This suggests that

minimum values possible for (1-cermet fraction) in the pin core are larger as is illustrated in the figures and Table 3.1-3. The absolute minimum core size is substantially greater for pin cores at the lower temperatures, with the variation between the two models decreasing with increase in temperature. Conversely, for similar fuels, fuel temperatures coolant pumping power and reactor power, the internally-cooled core allows substantial reductions in critical core diameter, volume, and weight at the lower temperatures.

3.2 OTHER RESULTS

3.2.1 Use of Figures

Figures I-4 and P-4 relate coolant pumping power and maximum fuel temperatures to a common parameter (1-cermet fraction) for 10 MW_t liquid metal-cooled cores fueled with $U^{235}O_2$, $U^{233}O_2$, and $Pu^{239}N$ embedded in a 50-50 vol% molybdenum matrix. Figure 5 gives pumping power values for various pressure ratios. Pumping power varies between 0-5 KW and the temperature from 2100-3000 °F. Various combinations of the two parameters (maximum fuel temperature and coolant pumping power) are possible to form a new base for comparisons, but values other than pressure ratios of 0.75, 0.85, 0.95, or 0.97 and maximum fuel temperature values of 2100, 2500, or 3000 °F require interpolation. Selection of these two parameters sufficiently defines (1-cermet fraction) for the three fuels

TABLE 3.1-3

ABSOLUTE MINIMUM VALUES (AS MITIGATED BY GEOMETRY CONSIDERATIONS) OF DIAMETERS, VOLUMES, AND WEIGHTS FOR INTERNALLY-COOLED AND FUEL PIN CRITICAL CORES FUELED WITH U^{235}, U^{233}, AND Pu^{239} 50 VOL% MOLYBDENUM CERMETS AT THREE MAXIMUM FUEL TEMPERATURES (L/D) = 1.0

Fuel	Temp. °F	Critical Core Diameter (ft)			Critical Core Volume (ft^3)			Critical Core Weight (lb)		
		Internally Cooled	Fuel Pin	Percent Increase	Internally Cooled	Fuel Pin	Percent Increase	Internally Cooled	Fuel Pin	Percent Increase
U^{235}	2100	1.22	1.40	15	1.40	2.15	54	780	1120	44
U^{233}	2100	.76	.97	28	.34	.72	112	230	350	52
Pu^{239}	2100	.61	.845	39	.18	.47	161	130	280	115
U^{235}	2500	1.20	1.285	7	1.40	1.66	19	770	880	14
U^{233}	2500	.745	.87	17	.32	.52	63	200	280	40
Pu^{239}	2500	.61	.745	22	.18	.32	77	130	200	54
U^{235}	3000	1.20	1.26	5	1.40	1.57	12	765	820	7
U^{233}	3000	.73	.84	15	.46	.46	53	220	250	14
Pu^{239}	3000	.61	.71	16	.28	.28	55	130	150	15

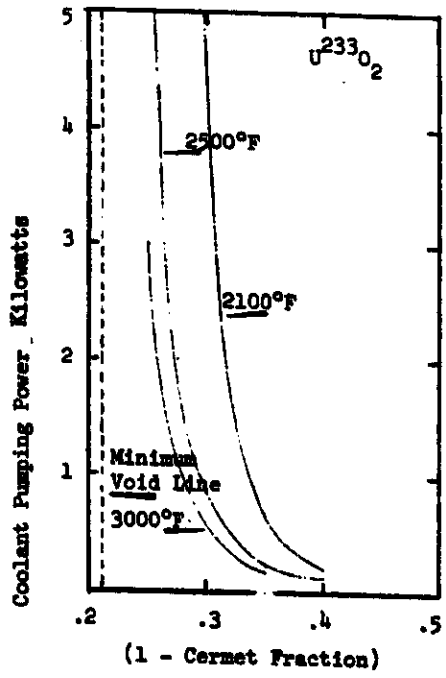

Coolant Pumping Power Versus (1 - Cermet Fraction) for Three Fuels $U^{235}O_2$, $U^{233}O_2$ and $Pu^{239}N$ Embedded in a 50 - 50 Vol % Molybdenum Matrix. Maximum Fuel Temperatures are:

2100°F = 1149°C
2500°F = 1371°C
3000°F = 1649°C

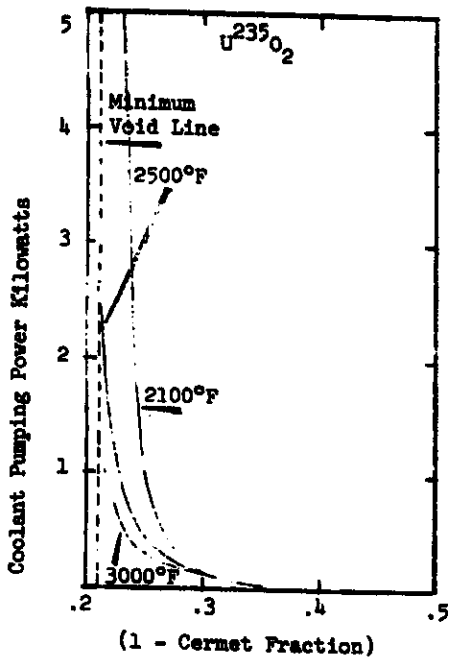

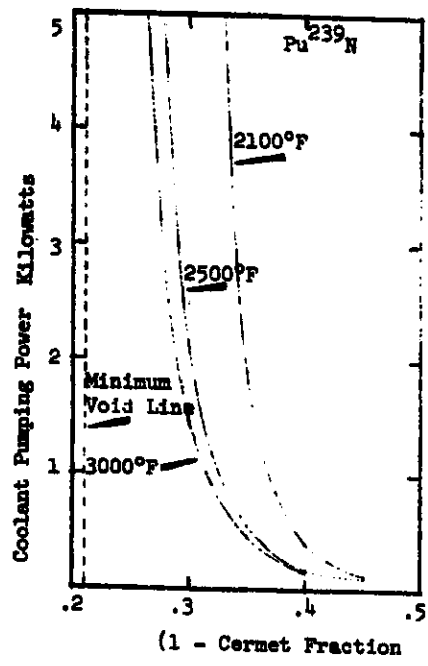

FIGURE I-4 Effect of (1 - cermet fraction) on Coolant Pumping Power for Internally Cooled Cores

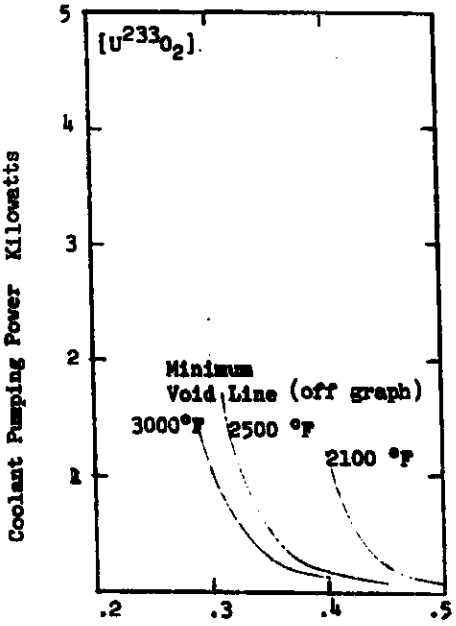

Coolant Pumping Power Versus (1 - Cermet Fraction) for three fuels, $U^{233}O_2$, and $Pu^{239}N$ embedded in 50-50 vol/% molybdenum matrix. Maximum fuel temperatures are are:

2100 °F = 1149 °C
2500 °F = 1371 °C
3000 °F = 1649 °C

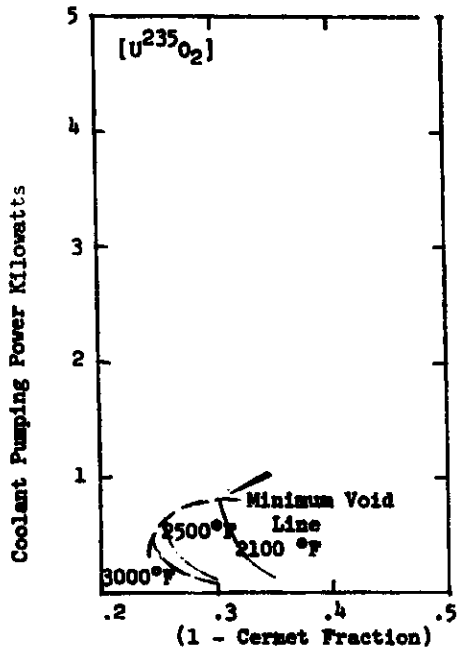

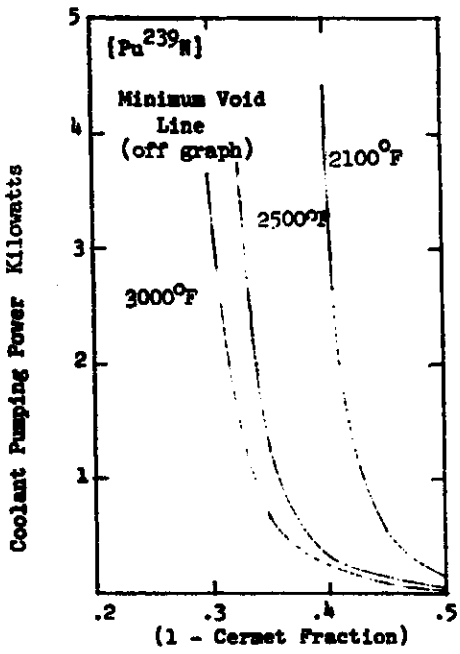

FIGURE P-4 Effect of (1 - cermet fraction) on Coolant Pumping Power for Pin Cores

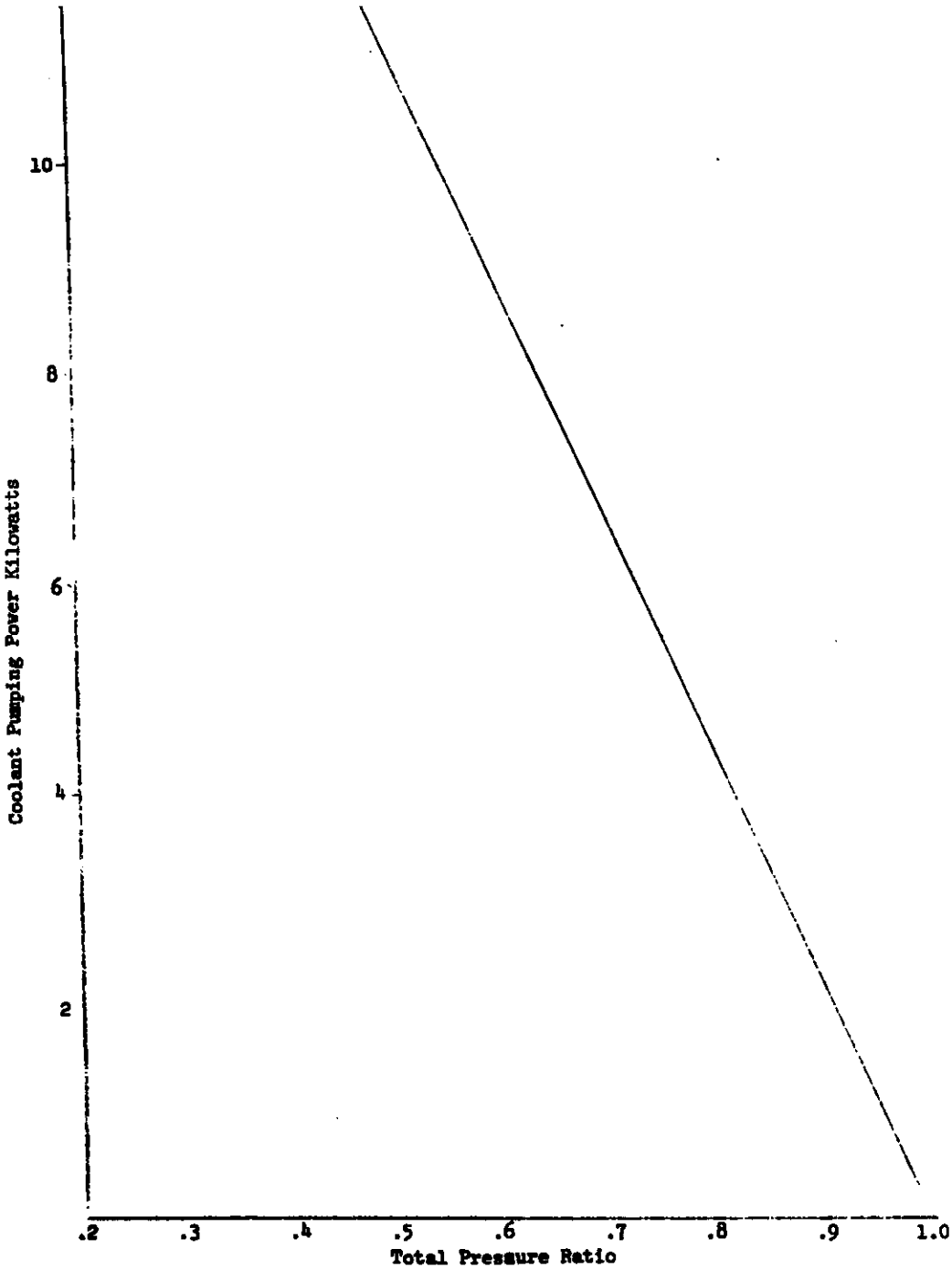

FIGURE 5 Effect of Total Pressure Ratio on Coolant Pumping Power for Inlet Pressures of 100 psi

considered from which 11 other parameters may be defined. Figures I-6, I-9, I-10, I-11, I-12 and I-13 and P-6 through P-13 correspond critical core values of hydraulic diameter, fuel diameter, wire diameter, exit velocity, average Reynolds number, equivalent number of coolant passages, and coolant and clad fraction for the various fuels and the two fuel geometries studied. For example, selection of a coolant pumping power of 650 watts and a maximum fuel temperature of 2100 °F with a reactor power specified at 10 MW_t defines (1-cermet fraction) to be 0.35, 0.259, and 0.384 for $U^{233}O_2$, $U^{235}O_2$, and $Pu^{239}N$, respectively in Figure I-4. Figure 5 shows the total pressure ratio to be 0.97 and associated with the above values of (1-cermet fraction), Figure I-6 gives hydraulic diameters of 0.104, 0.123, and 0.117 in. for the three fuels. Table 3.2-1 summarizes results for other parameters at 2100 °F fuel temperature and a pumping power of 650 watts (3 psi pressure drop).

3.2.2 Other Parametric Effects on Reactor Size and Weight

The hydraulic diameter, being fundamental to heat transfer was most useful in ascertaining tube* spacing and subsequently the quantity of fuel associated with each coolant channel. Changes in this fuel to coolant-channel ratio affects changes in fuel temperatures since the heat flux is also influenced by this ratio.

---

* Tubes refer to either coolant tubes for the internally-cooled core or fuel pins for the fuel pin core.

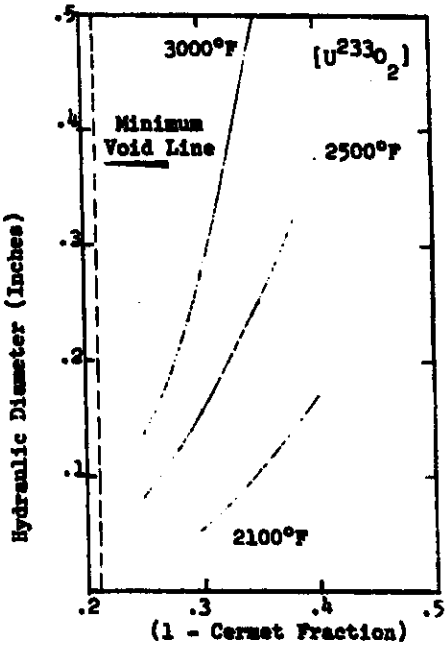

Hydraulic Diameter Versus (1 - Cermet Fraction) for three fuels, $U^{233}O_2$, and $Pu^{239}N$ embedded in a 50 - 50 vol/% molybdenum matrix. Maximum fuel temperatures are:

2100°F = 1149°C
2500°F = 1371°C
3000°F = 1649°C

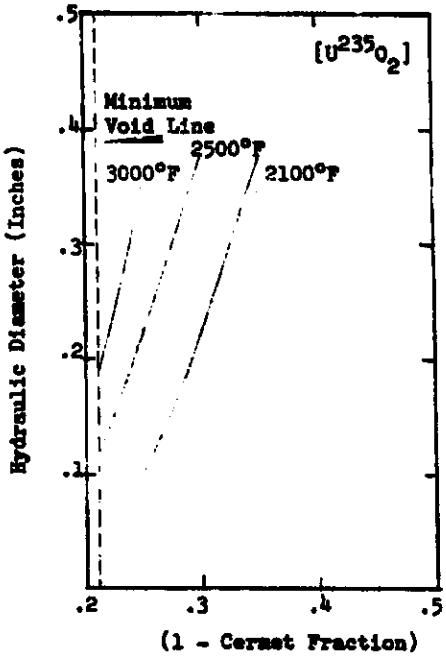

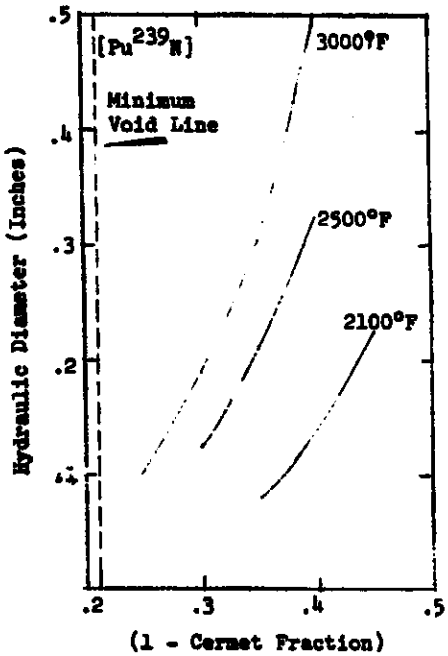

FIGURE I-6 Effect of (1 - cermet fraction) on Hydraulic Diameter for Internally Cooled Cores

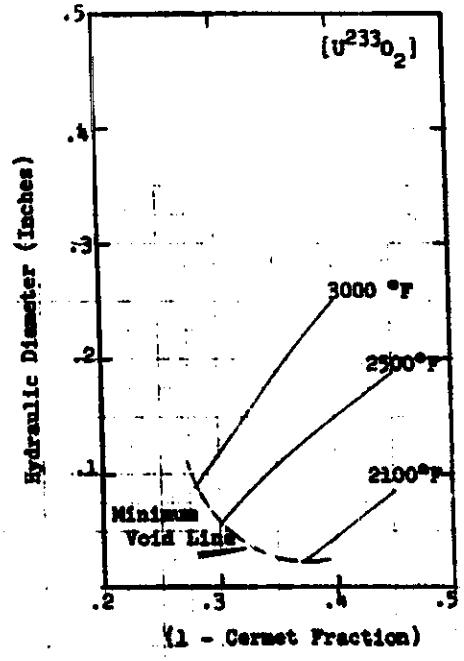

Hydraulic Diameter Versus (1 - Cermet Fraction) for Three Fuels, $U^{233}O_2$, and $Pu^{239}N$ Embedded in 50-50 vol/% Molybdenum Matrix. Maximum Fuel Temperatures are:

2100 °F = 1149 °C
2500 °F = 1371 °C
3000 °F = 1649 °C

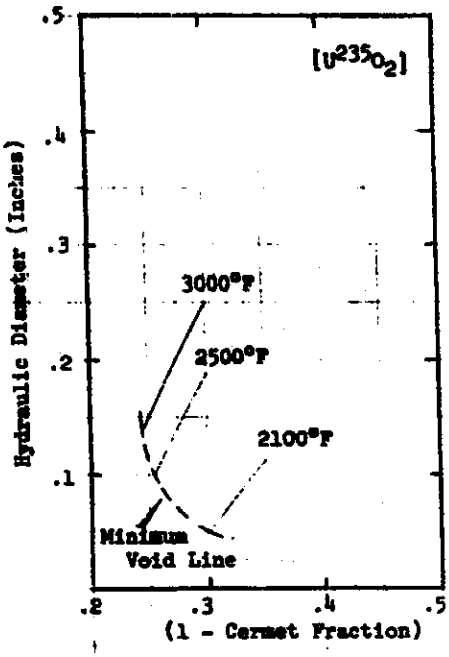

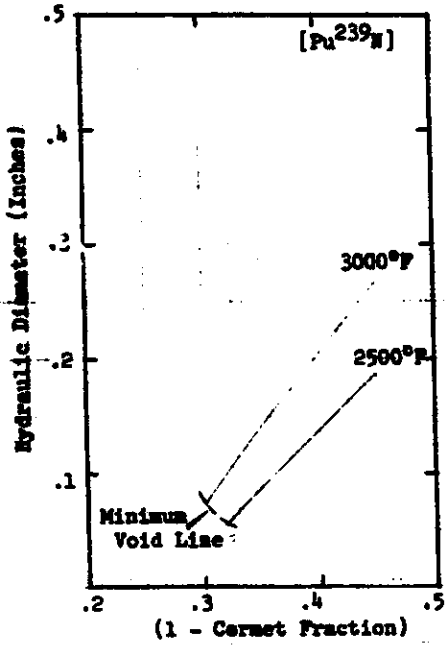

FIGURE P-6 Effect of (1 - cermet fraction) on Hydraulic Diameter for Pin Cores

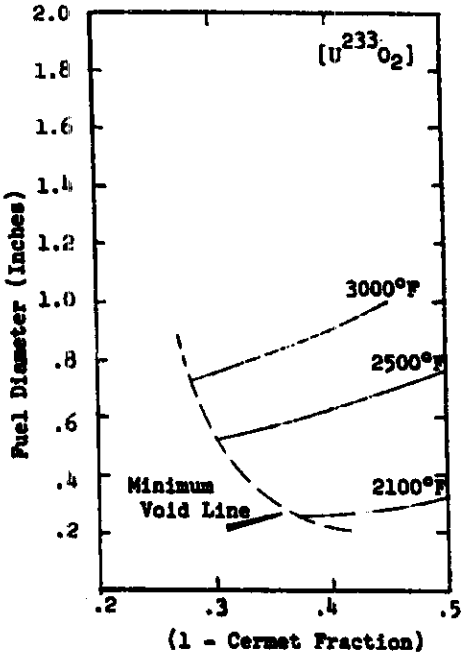

Fuel Diameter Versus (1 - Cermet Fraction) for Three Fuels $U^{233}O_2$, $U^{235}O_2$ and $Pu^{239}N$ Embedded in 50-50 vol/% Molybdenum Matrix. Maximum Fuel Temperatures are:

2100 °F = 1149 °C
2500 °F = 1371 °C
3000 °F = 1649 °C

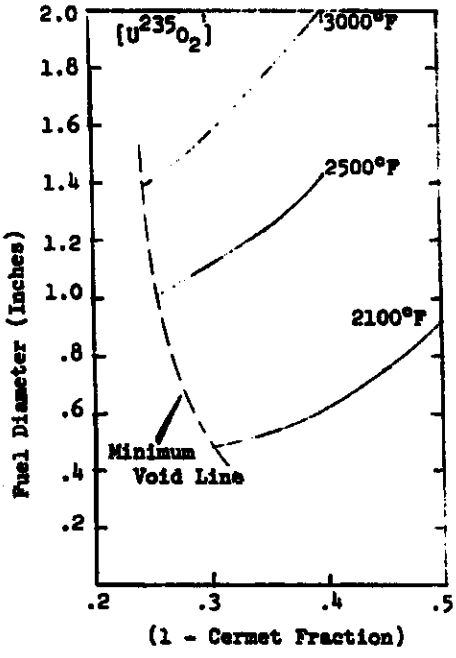

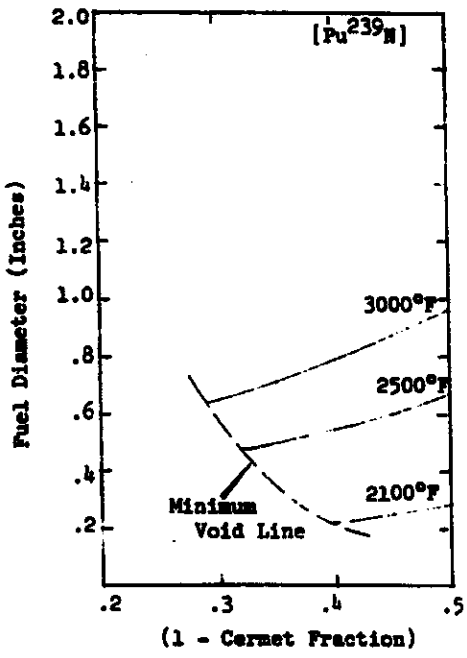

FIGURE P-7 Effect of (1 - cermet fraction) on Fuel Diameter for Pin Cores

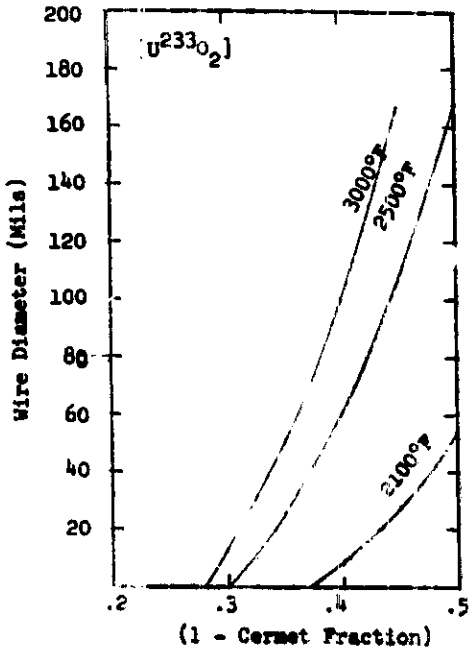

Wire Diameter Versus (1 - Cermet Fraction) for Three Fuels $U^{233}O_2$, $U^{235}O_2$, and $Pu^{239}N$ Embedded in 50-50 vol/% Molybdenum Matrix. Maximum Fuel Temperatures are:

2100 ° F = 1149 °C
2500 °F = 1371 °C
3000 °F = 1649 °C

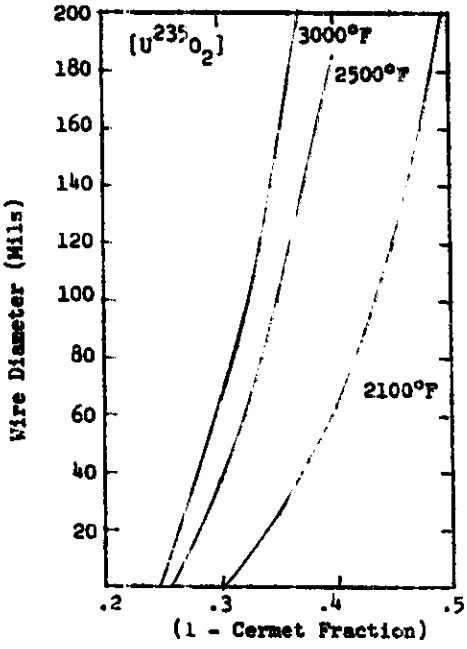

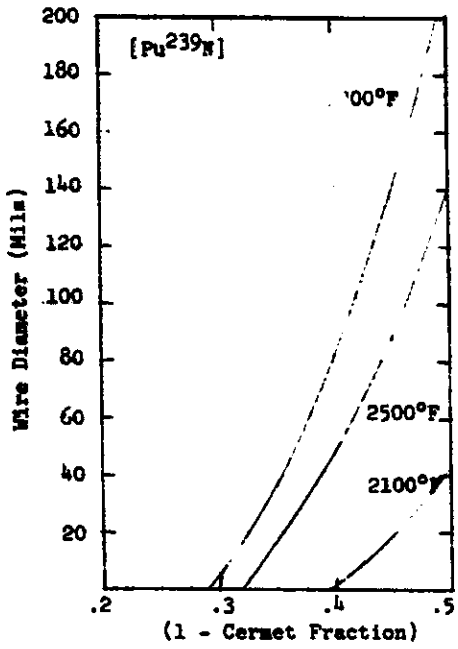

FIGURE F-8 Effect of (1 - cermet fraction) on Wire Diameter for Pin Cores

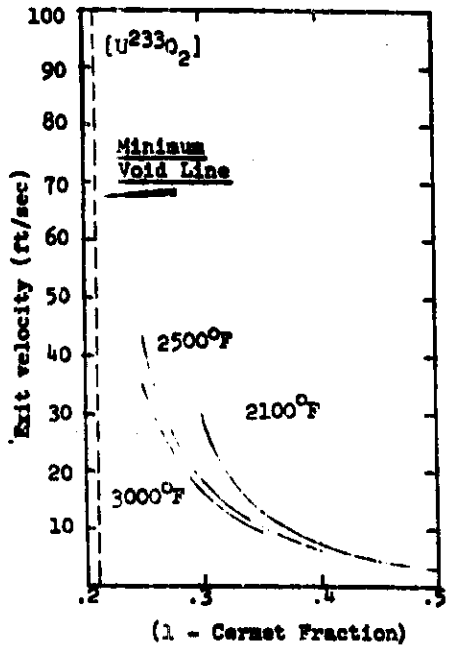

Exit Velocity Versus (1-Cermet Fraction) for Three Fuels, $U^{233}O_2$, $U^{235}O_2$, and $Pu^{239}N$ Embedded in a 50-50 vol% Molybdenum Matrix. Maximum Fuel Temperatures are:

2100 °F = 1149 °C
2500 °F = 1371 °C
3000 °F = 1649 °C

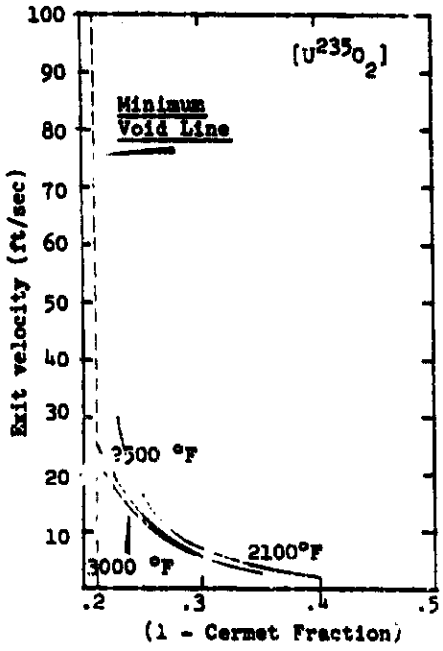

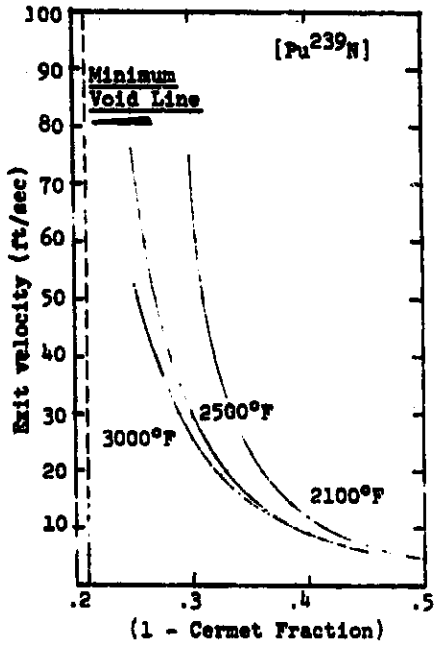

FIGURE I-9 Effect of (1 - cermet fraction) on Exit Velocity for Internally Cooled Cores

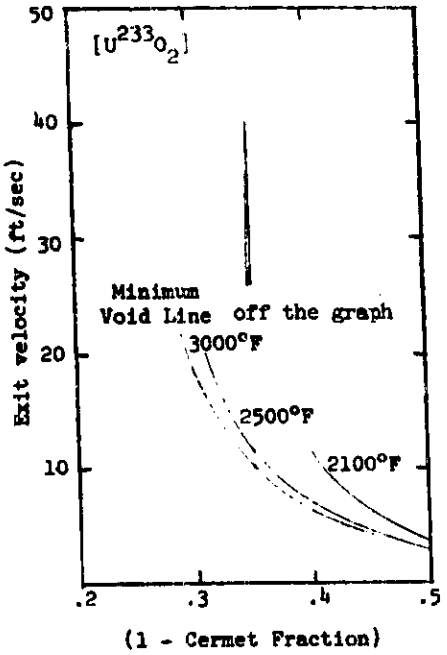

Exit Velocity Versus (1-Cermet Fraction) for Three Fuels, $U^{233}O_2$, $U^{235}O_2$, and $Pu^{239}N$ Embedded in a 50-50 vol% Molybdenum Matrix. Maximum Fuel Temperatures are:

2100 °F = 1149 °C
2500 °F = 1371 °C
3000 °F = 1649 °C

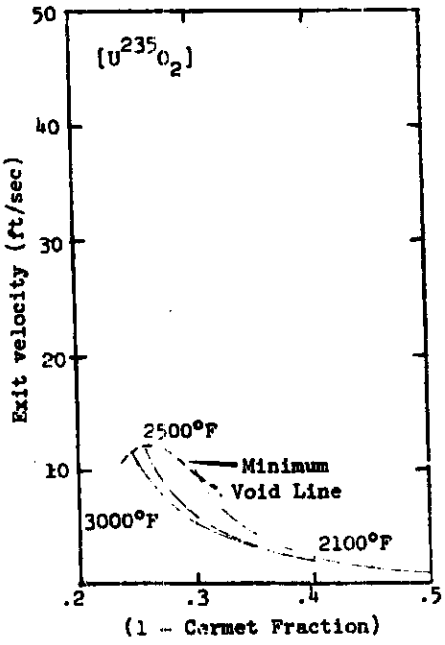

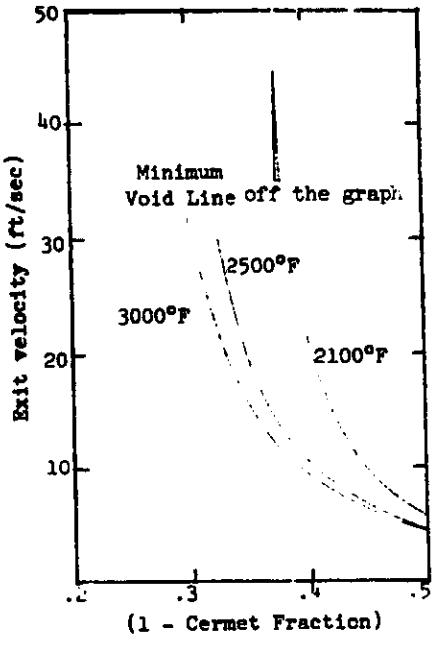

FIGURE P-9 Effect of (1 - cermet fraction) on the Exit Velocity for Pin Cores

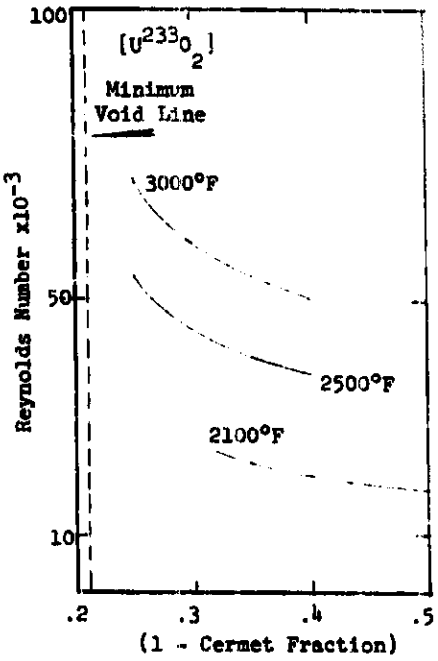

Reynolds Number Versus (1-Cermet Fraction) for Three Fuels, $U^{233}O_2$, $U^{235}O_2$, and $Pu^{239}N$, Embedded in a 50-50 vol% Molybdenum Matrix. Maximum Fuel Temperatures are:

2100°F = 1149°C
2500°F = 1371°C
3000°F = 1649°C

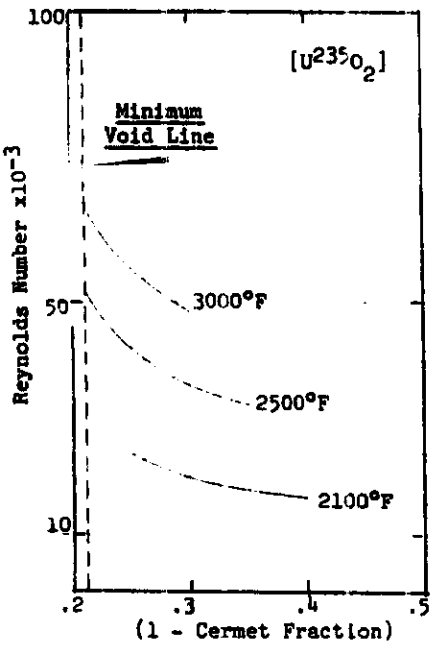

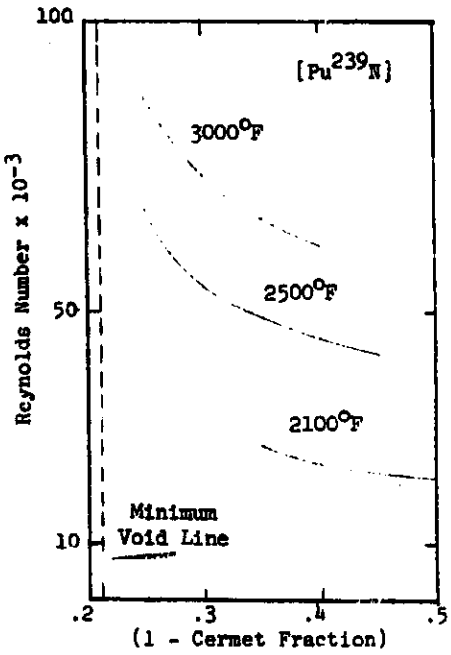

FIGURE I-10 Effect of (1 - cermet fraction) on Reynolds Number for Internally Cooled Cores

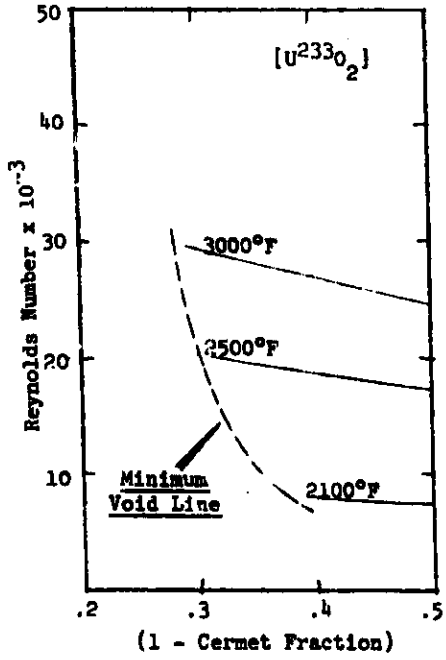

Reynolds Number Versus (1-Cermet Fraction) For Three Fuels $U^{233}O_2$, $U^{235}O_2$, and $Pu^{239}N$ Embedded in 50-50 vol% Molybdenum Matrix. Maximum Fuel Temperatures are:

2100°F = 1149°C
2500°F = 1371°C
3000°F = 1649°C

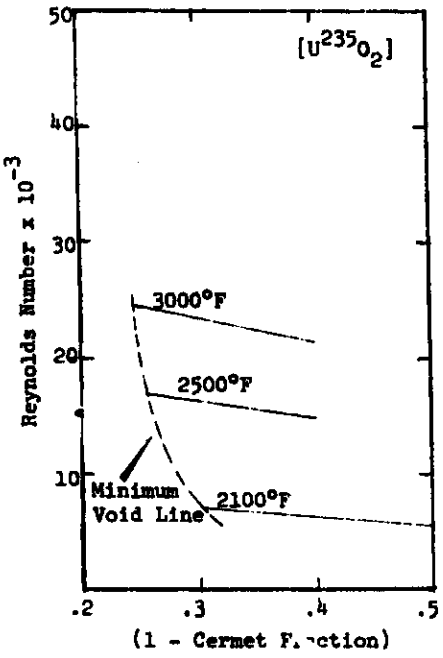

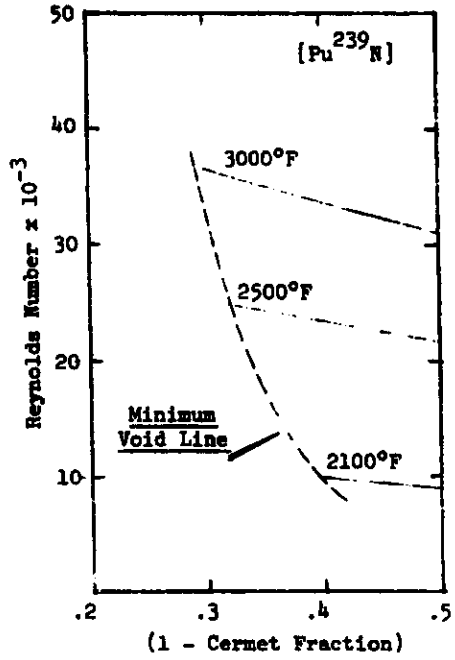

FIGURE P-10 Effect of (1 - cermet fraction) on Reynolds Number for Pin Cores

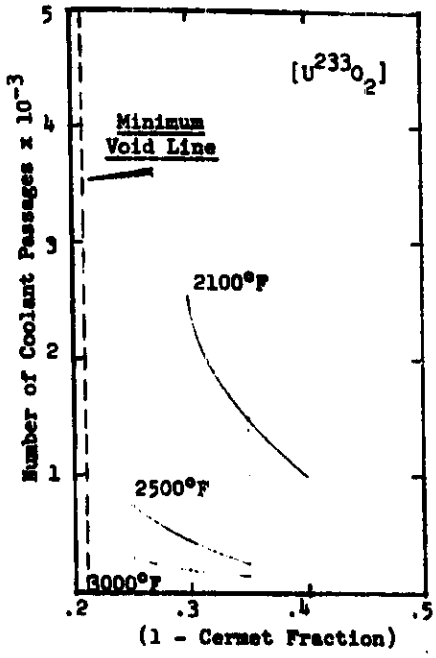

Total Number of Coolant Passages Versus (1-Cermet Fraction) for Three Fuels, $U^{233}O_2$, $U^{235}O_2$, and $Pu^{239}N$ Embedded in a 50-50 vol% Molybdenum Matrix. Maximum Fuel Temperatures are:

2100°F = 1149°C
2500°F = 1371°C
3000°F = 1649°C

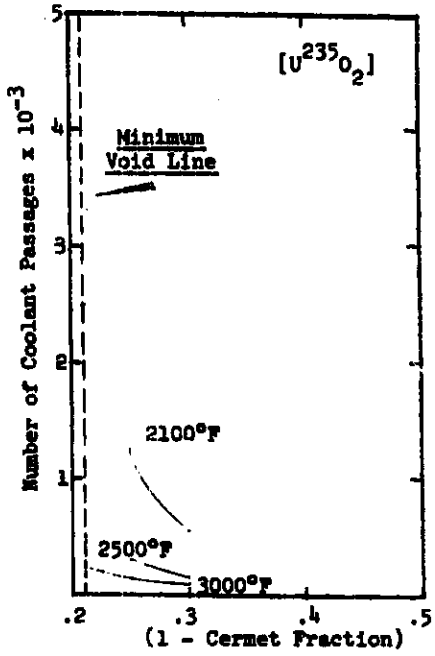

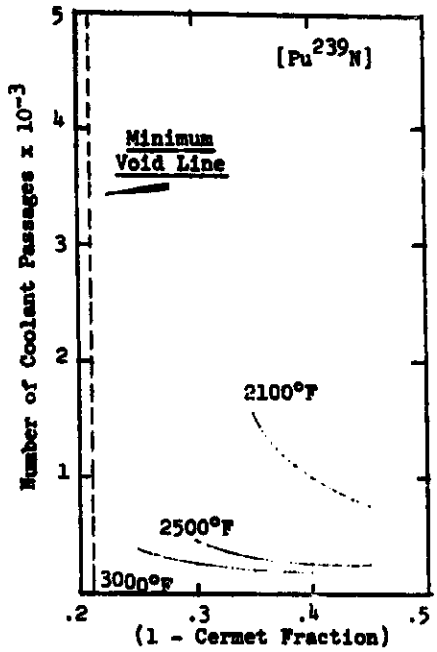

FIGURE I-11 Effect of (1 - cermet fraction) on the Number of Coolant Passages for Internally Cooled Cores

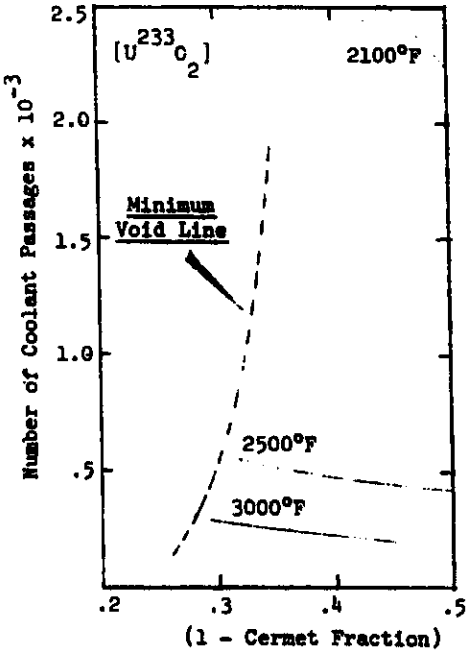

Total Number of Coolant Passages Versus (1-Cermet Fraction) for Three Fuels, $U^{233}O_2$, $U^{235}O_2$, and $Pu^{239}N$ Embedded in a 50-50 vol% Molybdenum Matrix. Maximum Fuel Temperatures are:

2100°F = 1149°C
2500°F = 1371°C
3000°F = 1649°C

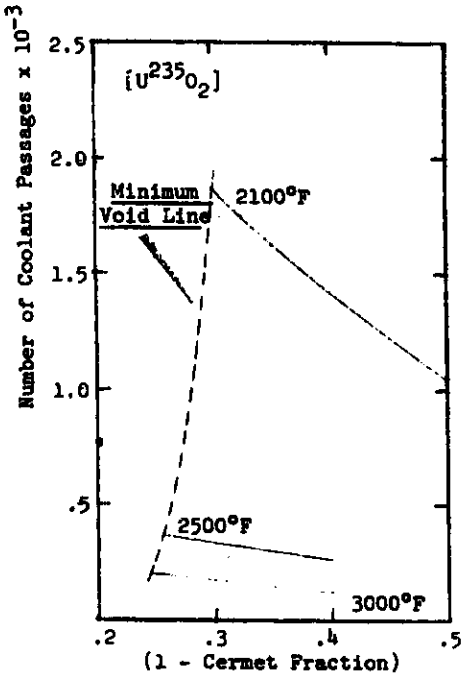

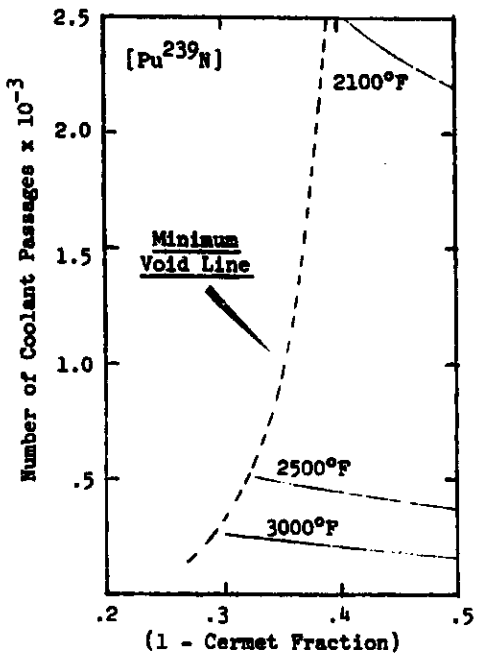

FIGURE P-11 Effect of 1 - cermet fraction) on the Number of Coolant Passages for Pin Cores

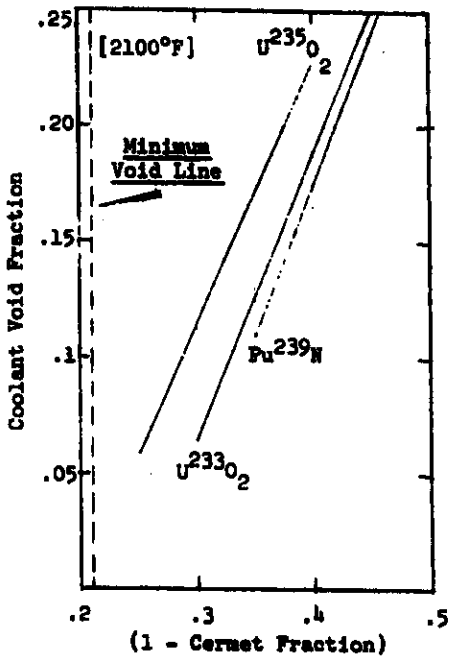

Coolant-Void Fraction Versus (1-Cermet Fraction) for Three Fuels, $U^{233}O_2$, $U^{235}O_2$, and $Pu^{239}N$ Embedded in a 50-50 vol% Molybdenum Matrix. Maximum Fuel Temperatures are:

2100°F = 1149°C
2500°F = 1371°C
3000°F = 1649°C

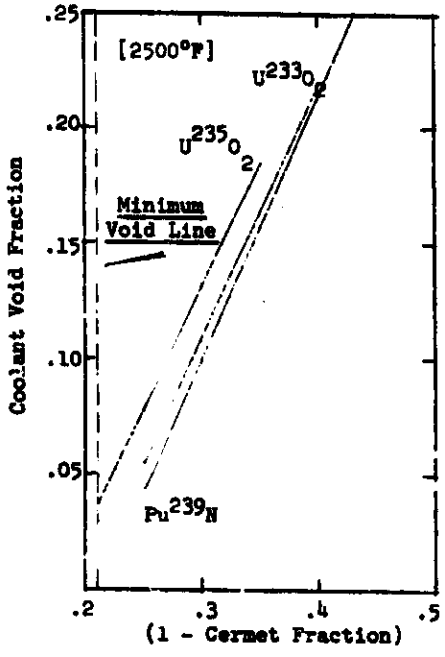

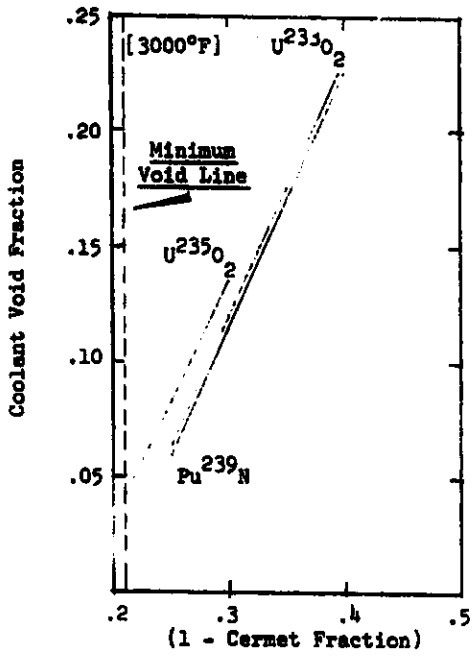

FIGURE I-12 Effect of (1 - cermet fraction) on the Coolant Void Fraction for Internally Cooled Core

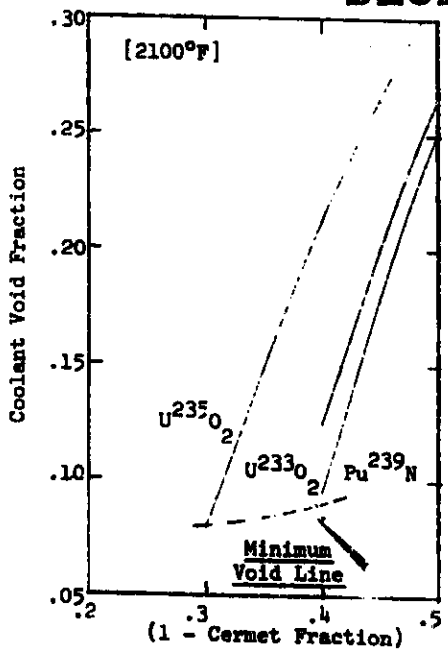

Coolant-Void Fraction Versus (1-Cermet Fraction) for Three Fuels, $U^{233}O_2$, $U^{235}O_2$, $Pu^{239}N$ Embedded in a 50-50 vol% Molybdenum Matrix. Maximum Fuel Temperatures are:

2100°F = 1149°C
2500°F = 1371°C
3000°F = 1649°C

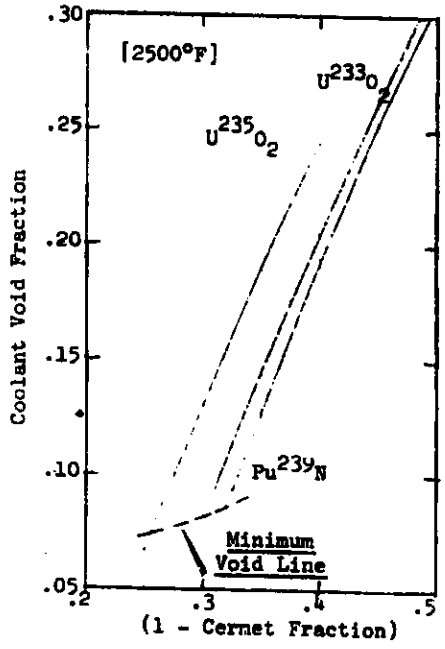

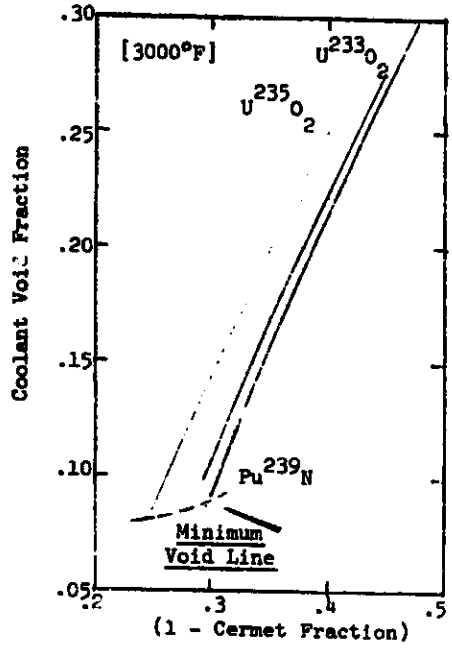

FIGURE P-12 Effect of (1 - cermet fraction) on Coolant Void Fraction for Pin Cores

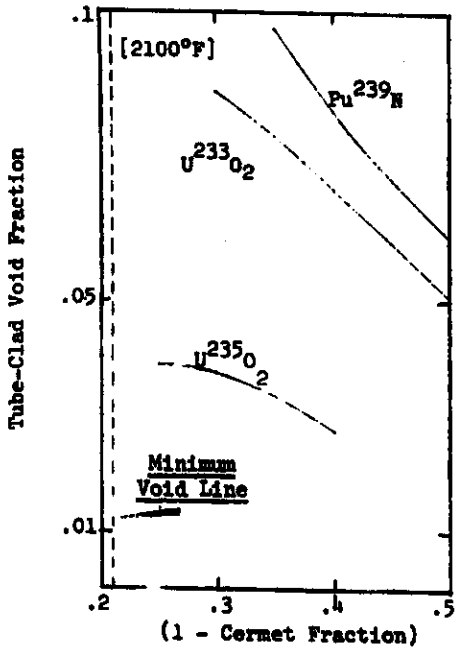

Tube-Clad Void Fraction Versus (1-Cermet Fraction) for Three Fuels, $U^{233}O_2$, $U^{235}O_2$, and $Pu^{239}N$ Embedded in a 50-50 vol% Molybdenum Matrix. Maximum Fuel Temperatures are:

2100°F = 1149°C
2500°F = 1371°C
3000°F = 1649°C

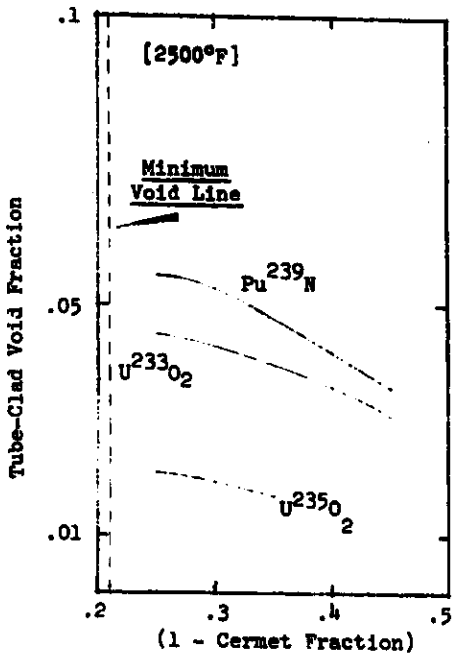

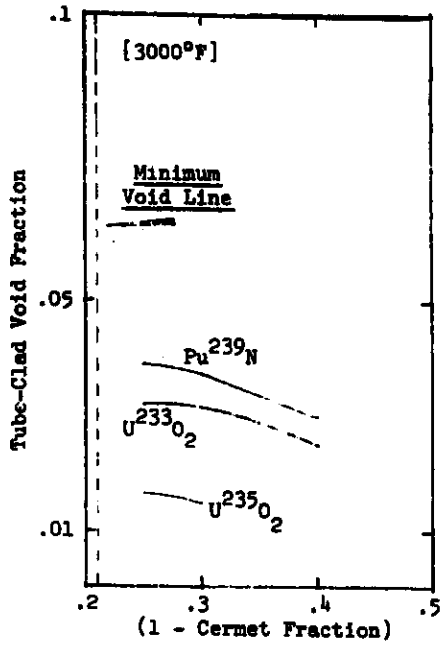

FIGURE I-13 Effect of (1-cermet fraction) on Tube-Clad Void Fraction for Internally Cooled Cores

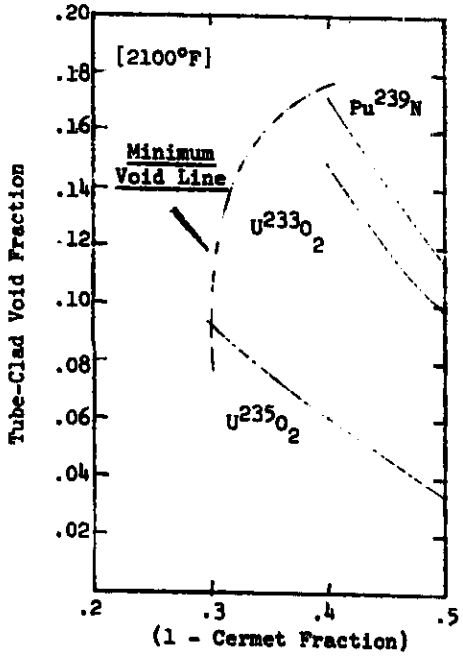

Tube-Clad Void Fraction Versus (1-Cermet Fraction) for Three Fuels, $U^{233}O_2$, $U^{235}O_2$, and $Pu^{239}N$ Embedded in 50-50 vol% Molybdenum Matrix. Maximum Fuel Temperatures are:

2100°F = 1149°C
2500°F = 1371°C
3000°F = 1649°C

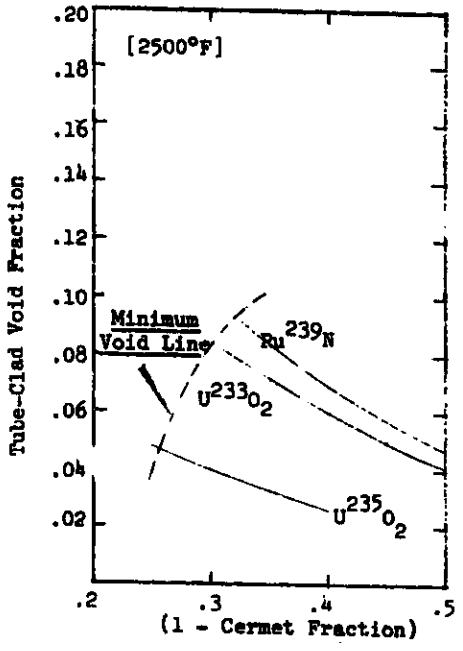

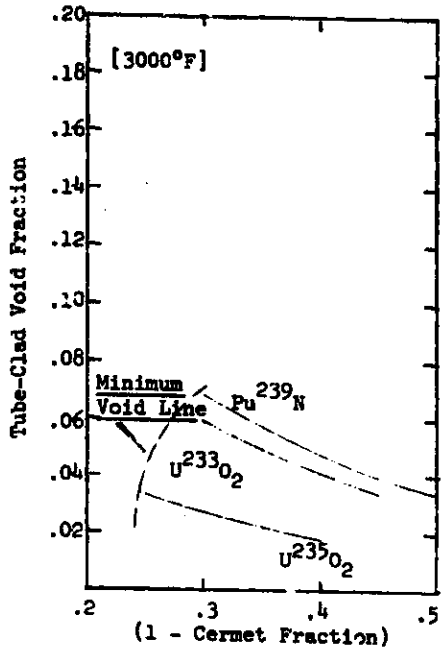

FIGURE P-13 Effect of (1-cermet fraction) on Tube-Clad Void Fraction for Pin Cores

TABLE 3.2-1

VALUES OF EIGHT DESIGN PARAMETERS FOR A FAST COMPACT LITHIUM-COOLED SPACE REACTOR FUELED WITH $U^{235}O_2$, $U^{233}O_2$, AND $Pu^{239}N$ EMBEDDED IN A 50 VOL% MOLYBDENUM MATRIX AND AT A MAXIMUM FUEL TEMPERATURE OF 2100 °F, A COOLANT PUMPING POWER OF 650 WATTS, AND A REACTOR POWER OF 10 MW_t

PARAMETER	$U^{235}O_2$		$U^{233}O_2$		$Pu^{239}N$	
	I *	P **	I	P	I	P
Tube Inside Diameter (in.)	.123	.49	.104	.262	.117	.25
Wire Diameter (in.)	--	.0025	--	.0135	--	.018
Exit Velocity (ft/sec)	13.2	8.2	13.0	8.3	14.2	10.3
Reynolds Number	23,000	7,100	22,000	7,900	24,500	9,500
Number Coolant Passages	490	1,830	1,480	2,692	1,110	2,355
Coolant Volume Fraction	.07	.087	.128	.153	.154	.17
Tube Clad Fraction	.039	.09	.0782	.136	.087	.1445
1 - Cermet Fraction	.259	.307	.35	.418	.384	.445

* (I) refers to an internally-cooled fuel geometry.

** (P) refers to a fuel pin core.

Therefore, to maintain a particular fuel temperature or heat flux at higher fuel ratios necessitates appropriate increases in hydraulic diameter. This is illustrated for several fuel temperatures in

Figure I-6, P-6, I-11, P-11 and P-7. I-6 and P-6 show the hydraulic diameter increasing with (1-cermet fraction); P-7 shows a similar behavior for the fuel diameter* in the fuel pin core, and I-11 and P-11 show the number of coolant channels to decrease with increases in (1-cermet fraction). These conditions satisfy the thermic equations and suggest that maintenance of a specific fuel temperature necessitates additional reactor size, weight, and space requirements when design pumping power limits do not influence optimal values for these parameters. Design pumping power also appears to be partially responsible for the additional size and weight of the fuel pin cores compared to the internally-cooled core. However, the primary reason for this additional size and weight is the thermal considerations influenced by the amount of heat to be removed and the equivalent distance it must travel in the two fuel geometries. Figure 14 illustrates the following geometrical relationship between the two models for a cermet fraction of 0.65:

- A 1 to 1 cermet ratio
- A 1 to 1 clad ratio
- A 1 to 1 coolant ratio**
- A 1 to 1 number of coolant channels per core ratio

These conditions were satisfied in the analytical conversion of the internally-cooled core at a given (cermet fraction) to the fuel pin model.

---

* Fuel diameter is defined to be the distance across the fuel in a fuel pin

** Valid only when wire wrap is excluded.

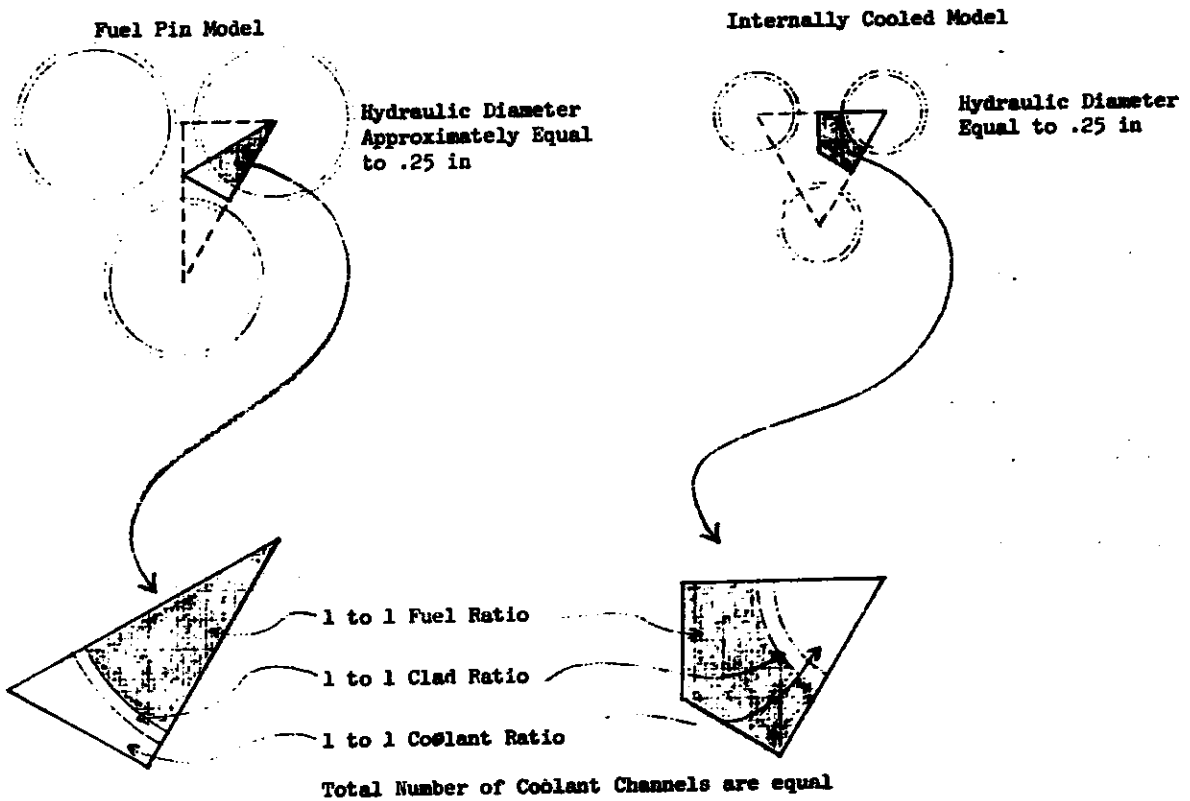

FIGURE 14 Geometric fuel-to-coolant relationship for internally-cooled and fuel pin reactor cores at a cermet fraction of .65. A 1 to 1 component volume ratio exists between the models. Wire wraps are not shown for the pin geometry.

A slight change in the hydraulic diameter occurs due to the thickness of the tube clad since one model uses the outer tube periphery for its calculation while the internally-cooled core uses the inner tube periphery to obtain its value. This would likely have an insignificant effect on the pressure drop and the maximum fuel temperatures between the two models. However, the smaller equivalent thermal conductance for the fuel pin was found to explain the higher fuel temperature for this model. To make the fuel temperatures equal in the two models requires reductions in the fuel diameter with a subsequent increase in the number of coolant channels, and hence pressure drop; or, to hold the pressure drop constant, an increase in (1-cermet fraction) with a subsequent increase in reactor size, weight, and space requirements. Add the additional pressure drop and fuel temperature resulting from wire wrap spacer considerations and the reason for higher fuel temperature in the pin core become evident. Values from I-11 compared to P-11 show the pin core to have more coolant channels at a similar maximum fuel temperature pressure ratio, reactor power and (1-cermet fraction) substantiating the above analysis.

Figure P-8 illustrates the effect of (1-cermet fraction) on the diameter of the wire spacer for the three fuels at several maximum fuel temperatures. As (1-cermet fraction) increases, the wire diameter increases which would effect an increase in coolant pumping

power should the hydraulic diameter remain constant. However, as shown above, there are also increases in both the pin diameter and the hydraulic diameter and therefore a net decrease in pressure drop accompanies an increase in (1-cermet fraction). This is illustrated in Figure P-4 and Figure 5. Since the wire diameter does increase with (1-cermet fraction), a larger change in this fraction is necessary to maintain a constant value for the coolant pumping power. Thus, additional core size and weight is influenced for this fuel geometry.

3.2.3 Effect of Coolant Velocities and Reynolds Number on Reactor Size

Figures I-9 and P-9 illustrate the effect of (1-cermet fraction) on coolant exit velocity for several molybdenum cermets and at three maximum fuel temperatures. Similar velocities for the fuels indicate a requirement of greater values for (1-cermet fraction) in the alternate more fissile fuels. Inspection of the figures also illustrates that exit velocities are very nearly the same for similar coolant pumping power, maximum fuel temperature, and reactor power for a particular fuel geometry. For this condition to exist, the total core cross-section area containing coolant for the three fuels must be similar. Substantiation of this can be demonstrated from the continuity equation since the coolant flow rate ($\dot{\omega}$) and the exit coolant density are the same for all the fuels at similar inlet conditions, fuel temperatures and reactor power. Also, the condition imposed by a similar coolant

pumping power, is that the frictional surfaces (total wetted perimeter) be the same for all the fuels at similar coolant velocities. Further, the higher power density of the alternate more fissile fuels requires a higher coolant to fuel ratio to maintain similar maximum fuel temperature. Therefore, the necessity for greater values of (1-cermet fraction), for $U^{233}O_2$ and $Pu^{239}N$ fuels is evident, and similarity in exit velocity would be an expected result.

Variation in the exit velocity does exist between the two models as is illustrated in Figures I-9 and P-9. The internally-cooled core requires higher velocities than the pin model, which suggests the pin model has a larger core cross-section containing coolant for a constant flow rate than the internally-cooled core. The explanation for this condition is found in the thermal analysis of the two cores described in Section 3.2.2 and Figure 14. The pin core requires larger (1-cermet fraction) values under the conditions imposed for fuel and fuel-geometry comparisons and therefore a larger core area is devoted to coolant which results in a lower exit velocity. Figure I-12 and P-12 illustrate the coolant void fraction of the core as a function of (1-cermet fraction) and results indicate larger coolant voids accompany increases in the fraction.

The exit velocity is also a measurement of the Reynolds number. Figure I-10 and P-10 illustrate the effect of (1-cermet fraction) on the average Reynolds number. The figure shows the validity of

the assumption that turbulent flow exists through the core and hence verifies the applicability of the equations used describing heat removal.(7) The pin core evidences large reductions in Reynolds number at similar pressure ratios and maximum fuel temperatures compared to the internally-cooled model.

Coincident to the coolant velocity and Reynolds number, the number of coolant channels also experiences increases in number with decreases in (1-cermet fraction). This is illustrated in Figure I-11, P-11 and I-12 for the two models. This is an expected result based on the analysis made in Section 3.2.2 with respect to the fuel per coolant channel ratio and thermic considerations. It also follows that as the velocity increases, the core cross-section area containing coolant also decreases to maintain a constant flow rate, fuel temperature, and coolant pumping power.

4.0 Conclusions

- Use of the more fissile fuels allows a substantial reduction in core size, space and weight requirements with no additional expense in pumping power or maximum fuel temperature.

- Increase in maximum fuel temperature allows reduction in core diameter, volume, and weight. $U^{235}O_2$-fueled cores show greater change than the alternate more fissile fuels and require large

core volumes at temperatures above 2100 °F which are not heat transfer limited. This may be an important factor in evaluating the three fuels when endurance limits are considered.

- Internally-cooled cores allow reductions in reactor core size, space, and weight requirements at similar coolant pumping power, maximum fuel temperature, and reactor power due to geometry effects.

- Sufficient identification is made of lithium-cooled fast compact reactor critical cores fueled with $U^{235}O_2$, $U^{233}O_2$, and $Pu^{239}N$ embedded in a 50 vol% molybdenum matrix to facilitate the planned transient analysis.

APPENDIX A

THERMAL AND HYDRAULIC PARAMETERS

A-1 COOLANT PROPERTIES

The coolant selected for this study is liquid lithium. Its low density, high specific heat and vapor pressure qualities make it especially attractive to heat transfer applications. A highly corrosive nature presents problems of containment. However, 1-columbium 0.1-zirconium-alloy has safely resisted corrosion for 10,000[8] experimental operating hours at conditions typical of those in nuclear reactors.

Lithium properties versus temperature are not so readily available as properties of sodium and potassium. Weatherford and Tyler[9] F. J. Tebo[10] Pratt and Whitney[8], and the Liquid Metals Handbook,[11] give values for the metal. The experimental effort of Pratt and Whitney suggests that confidence can be place in these data and consequently the coolant properties are based thereon. However, when these data were lacking, Weatherford and Tyler data are used. Figure A-1 through A-5 show values of vapor pressure, viscosity, thermal conductivity, density, and specific heat versus temperature. The solid lines represent Pratt and Whitney data, the dotted lines Weatherford and Tyler. Table A-1 shows coolant conditions selected for the study.

TABLE A-1

	Inlet	Outlet
Temperature	1,700	2,000
Pressure psia	100	Varied
Coolant flow rate lb/sec	31.94	31.94
Film coefficient	32,000	32,000

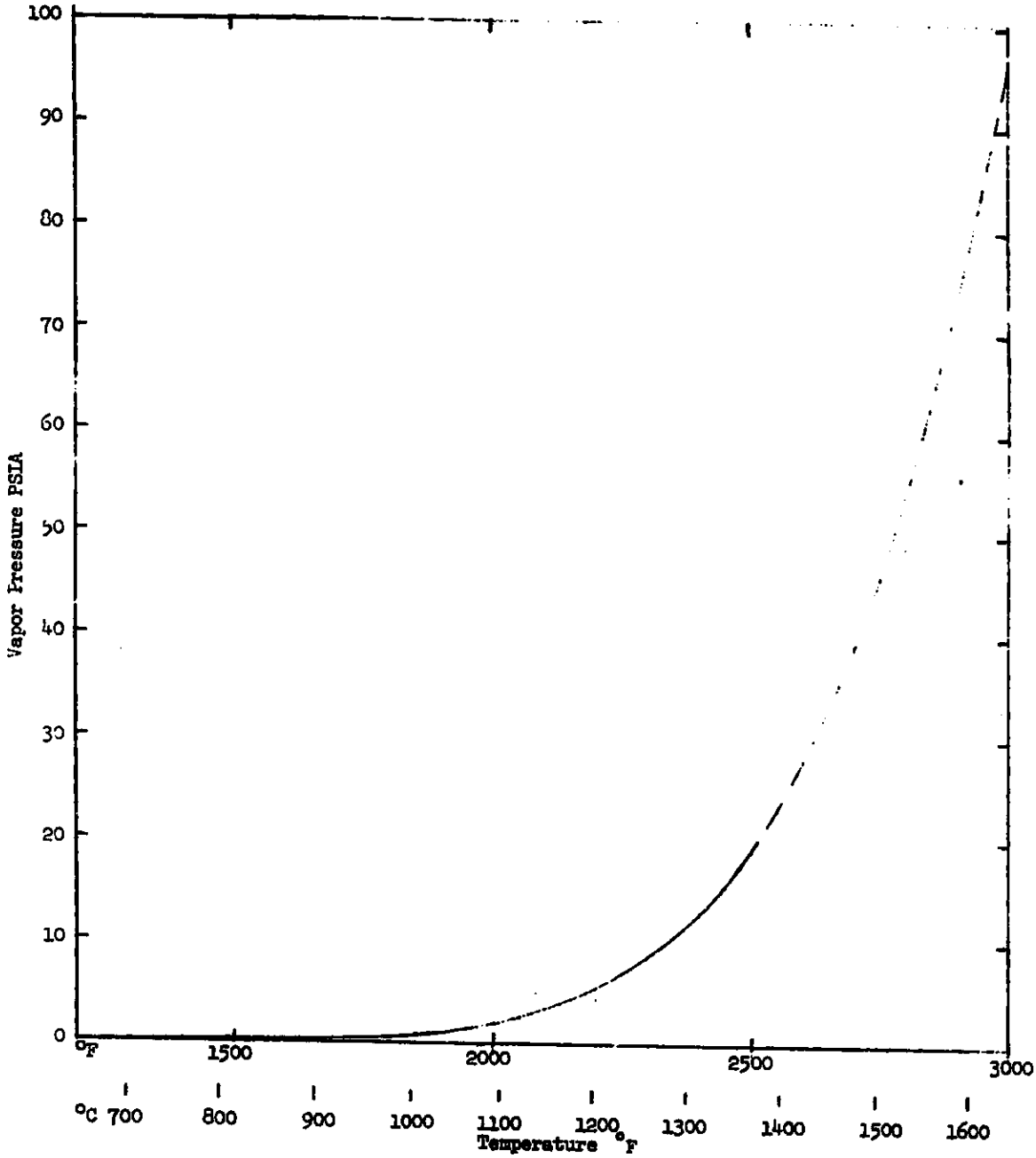

FIGURE A-1 Vapor Pressure of Lithium

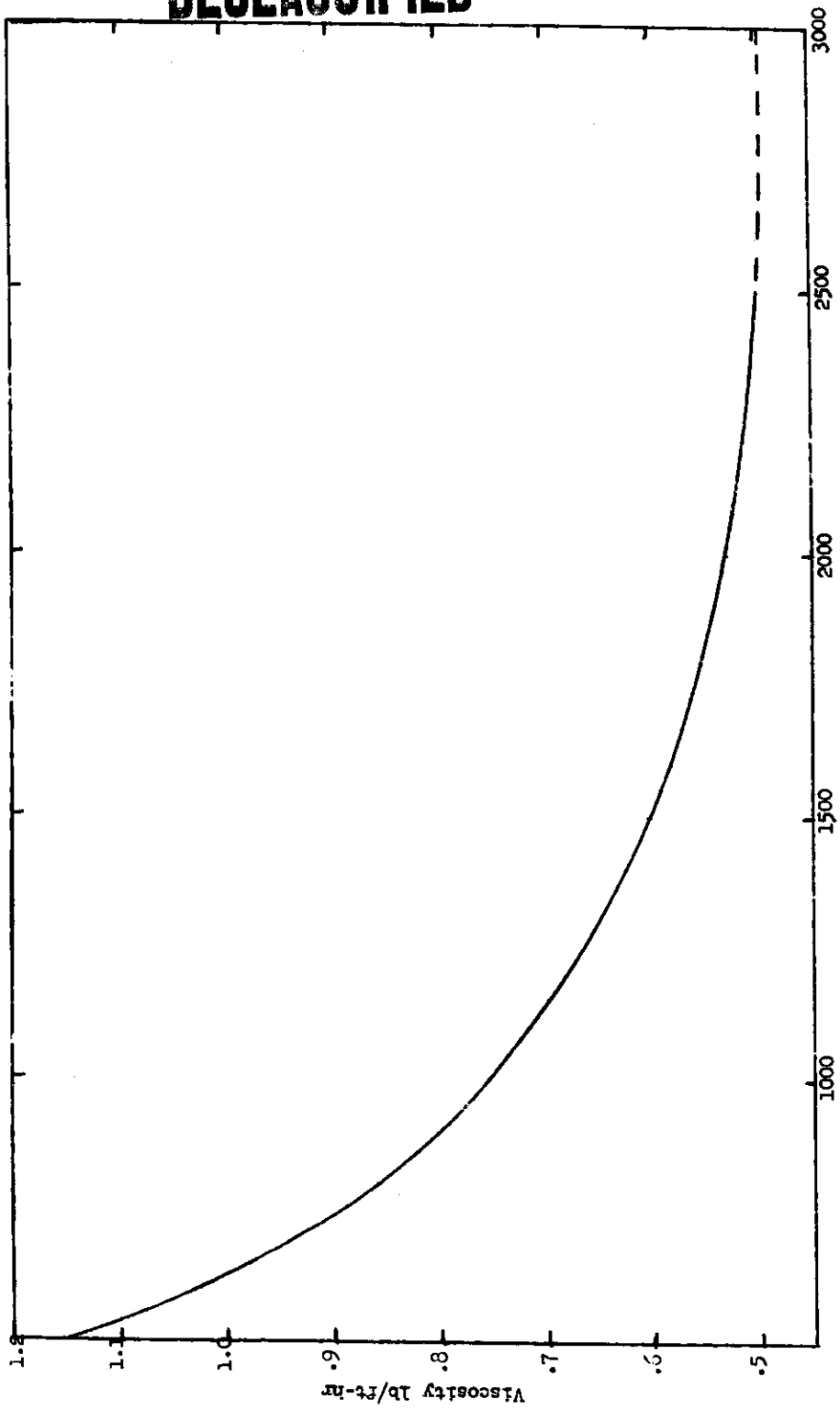

FIGURE A-2 Viscosity of Lithium

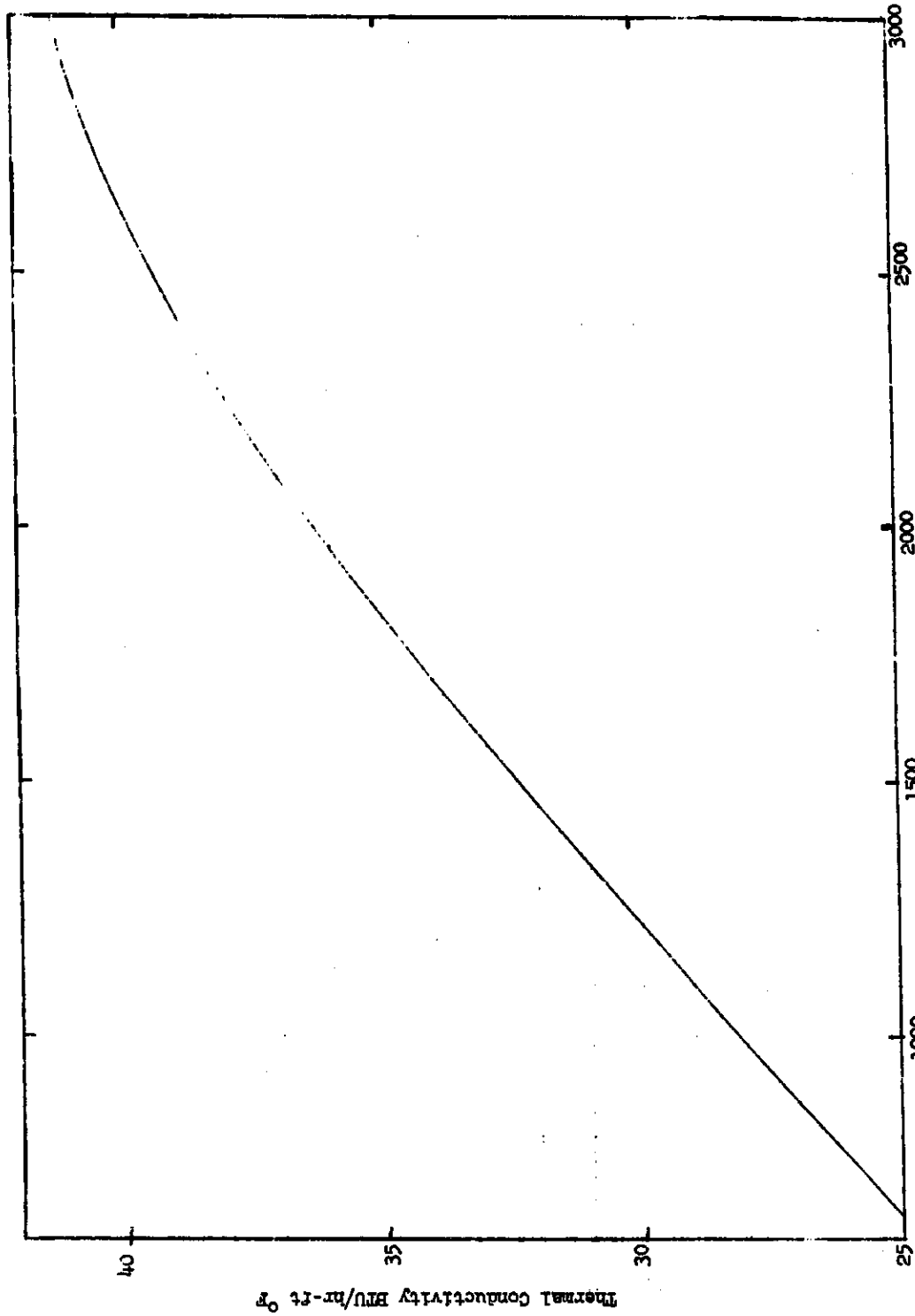

FIGURE A-3 Thermal Conductivity of Lithium

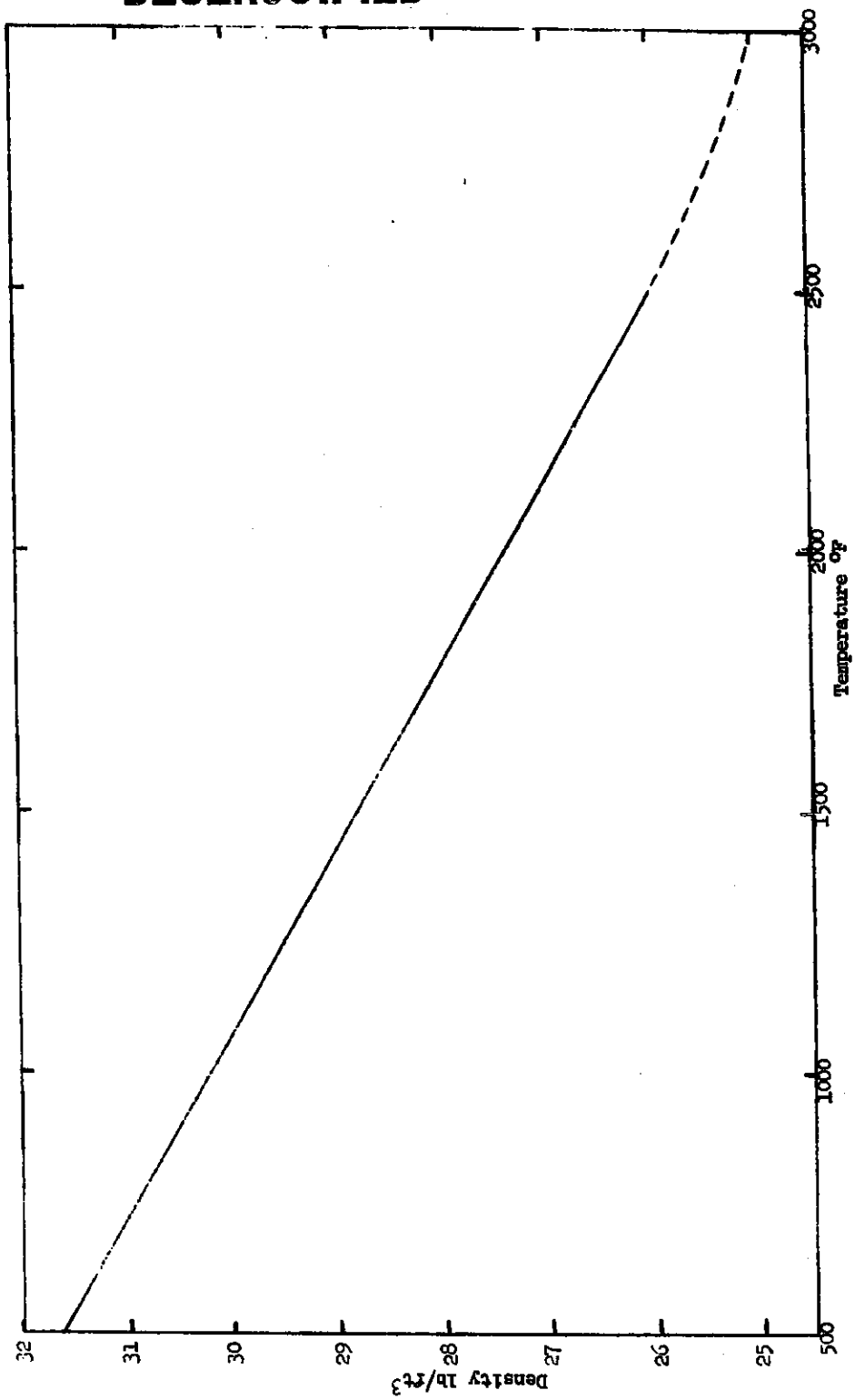

FIGURE A-4 Density of Lithium

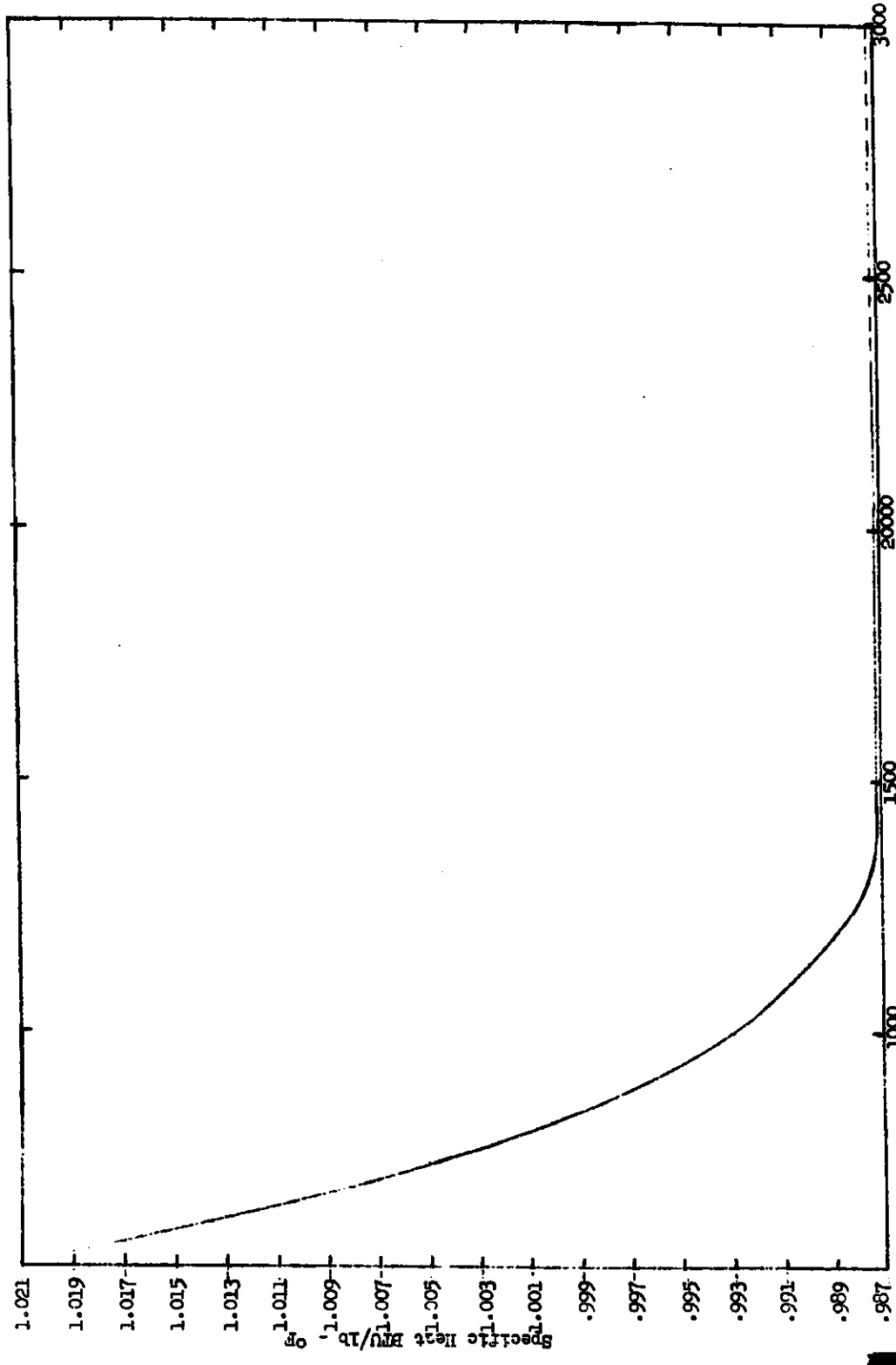

FIGURE A-5 Specific Heat of Lithium

The film coefficient (32,000) is considered reasonable and is a constant value. An exit pressure of 2 psia assures saturation conditions at the 2000 °F exit temperature and therefore an inlet pressure of 100 psia is sufficient to maintain liquid phase coolant conditions for pressure drops of interest.

B-2 PRESSURE DROP

Pressure drop calculations for the internally-cooled core presents no problem since conventional equations are applicable. The addition of wire spacers in the pin model, though highly desirable as coolant mixing promoters, substantially increase the pressure drop in the coolant stream. Some experimental work is available in determining the loss (References 6, 12, 13, 14, 15). E. D. Waters[6] suggests a pressure drop ratio equation which closely approaches experimental values. This relationship is:

$$\frac{\Delta P_w}{\Delta P_n} = N + Nn^2$$

where

ΔP_w = static pressure drop in channels containing wire spacers.

ΔP_n = static pressure drop in channels containing no wire spacers but with the same pin spacing.

N = ratio of the static pressure drop in channel with a wire placed axially along the pin (no wrapping) and ΔP_n.

M = 2.153 times the wire diameter.

n = number of wire revolutions per unit length of rod.

Since the quantities ΔP_n, N, M, and n are calculable, an expression for ΔP_w is obtained. Two limitations are:

(1) n should not be less than 6 wraps per foot.

(2) valid for wire sizes between 88 and 138 mils.

Limitation #2 could possibly be less restrictive since the range of experimental data available were bracketed by these values and therefore the validity of the expression outside this limit is not known. For purposes of this report, the assumption is made that this limitation does not apply.

B-3 FRICTION FACTOR

The friction factor used is that found in the literature for smooth pipes.[5] The pin model required additional effort since pressure drop calculations made are with and without wire spacers. Since the presence of wire reduces the available coolant channel area, the velocities increase to accommodate the same flow rate and affect the friction factor. ΔP_n and N are evaluated using a friction factor pertaining to its unique condition. The code as written for the internally-cooled core facilitates calculation of that portion of N which pertained to the pressure drop in a channel with wire placed axially along the pin but modification was necessary for ΔP_n. The following equations are added for this achievement. The subscript u signifies conditions without the presence of wire.

$$A_u = \frac{D_h C}{4} + \frac{\pi D_w^2}{8}$$

$$C_u = \frac{\pi(D_p + 2tc)}{2}$$

$$D_{hu} = \frac{4A_u}{C_u}$$

$$G_u = \frac{W}{N_c A_u}$$

$$V_{1u} = \frac{G_u}{3600\ \rho_1}$$

$$V_{2u} = \frac{G_u}{3600\ \rho_1}$$

where:

A = cross section area of coolant passage

C = wetted perimeter

D_h = hydraulic diameter

G = mass flow rate

V_1 = inlet velocity

V_2 = exit velocity

APPENDIX B

FUEL PROPERTIES

B-1 FUELING

The three fuels considered consist of $U^{235}O_2$, $U^{233}O_2$, and $Pu^{239}N$ embedded in a 50 vol% molybdenum matrix. Selection of molybdenum as the fuel diluent was made in an effort to lower fuel temperatures and density. Since the criticality curves were those of a tungsten matrix, assumption was made that changing to molybdenum will not invalidate these curves.

The heat transfer calculations were based on a model containing cermet fuel at 100% theoretical density. Since the real model contains 5% void space in the fuel matrix, a corrected thermal conductivity for the heat transfer model was necessary. Properties for the cermets were not readily available and hence corrected thermal conductivity values were calculated from the Maxwell equation:(16)

$$\frac{ka}{ks} = \frac{1-(1-a\frac{kp}{ks})b}{1+(a-1)b}$$

where

ka = apparent thermal conductivity in the mixture

kp = thermal conductivity of particulate matter (fissile material).

ks = thermal conductivity of the fuel diluent.

$$a = \frac{3ks}{2ks + kp}$$

$$b = \frac{Vp}{Vs + Vp}$$ (volume fraction of particulate matter)

The thermal conductivities for fuel constituents is taken from References 17, 18 and 19 and for convenience are reproduced in Figure B-3, B-4 and B-5. Resulting cermet thermal conductivities are shown in Figure B-1 and B-2. Discretion should be used when applying these values to cermets with greater fuel void than defined herein.

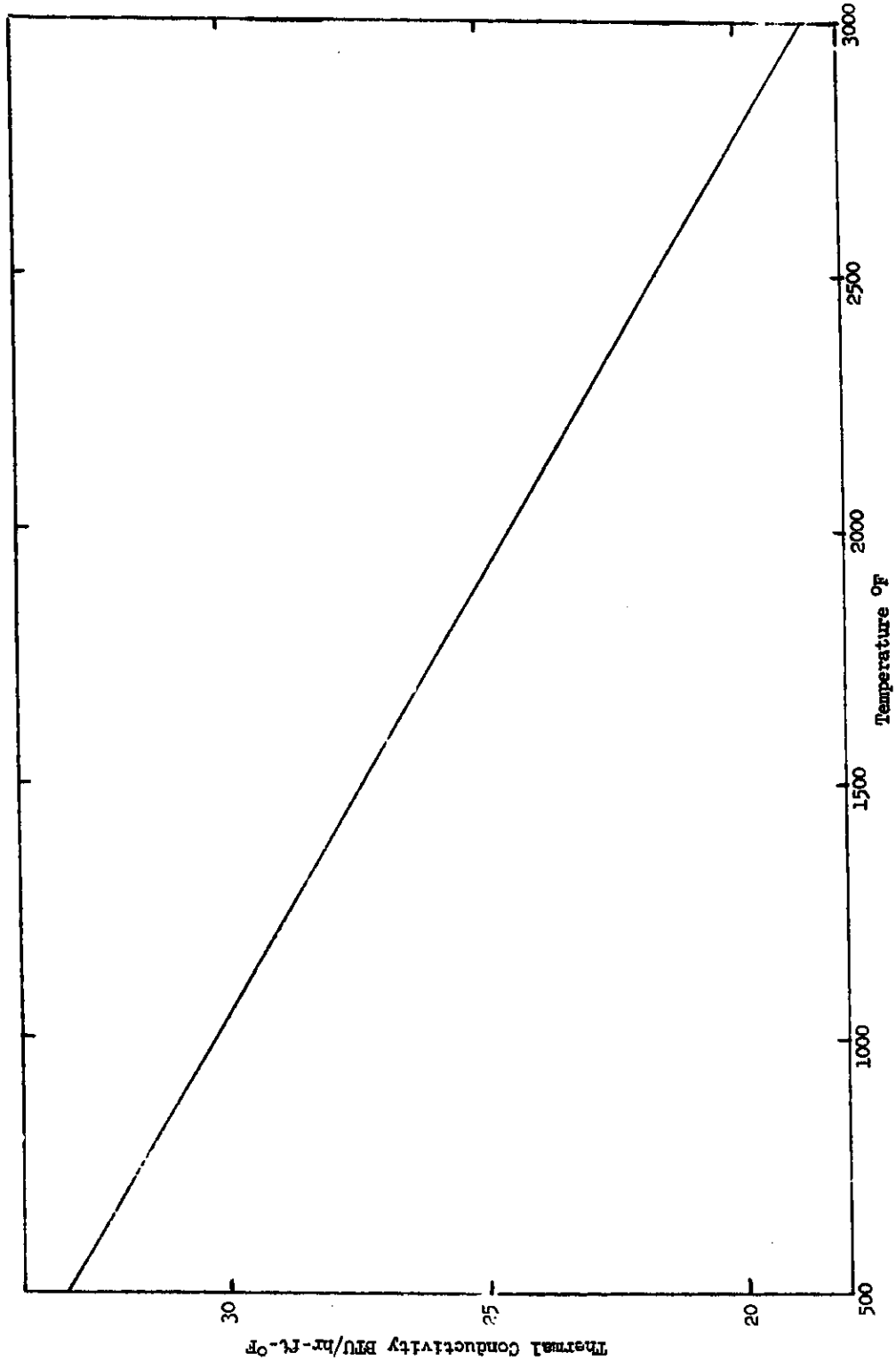

FIGURE B-1 Thermal Conductivity of UO_2-Molybdenum Cermet (50-50 vol%)

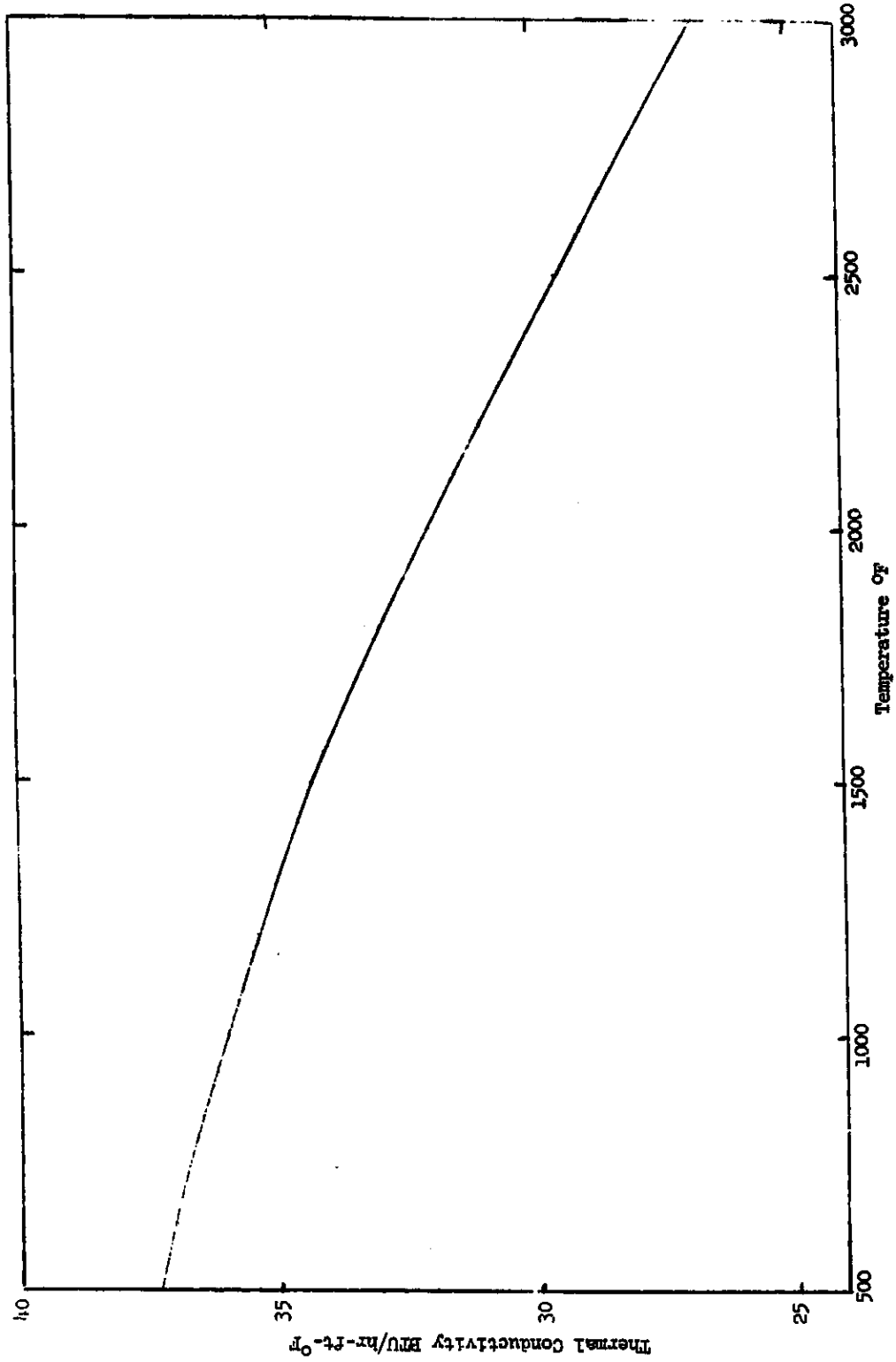

FIGURE B-2 Thermal Conductivity of PuN-Molybdenum Cermet (50-50 vol%)

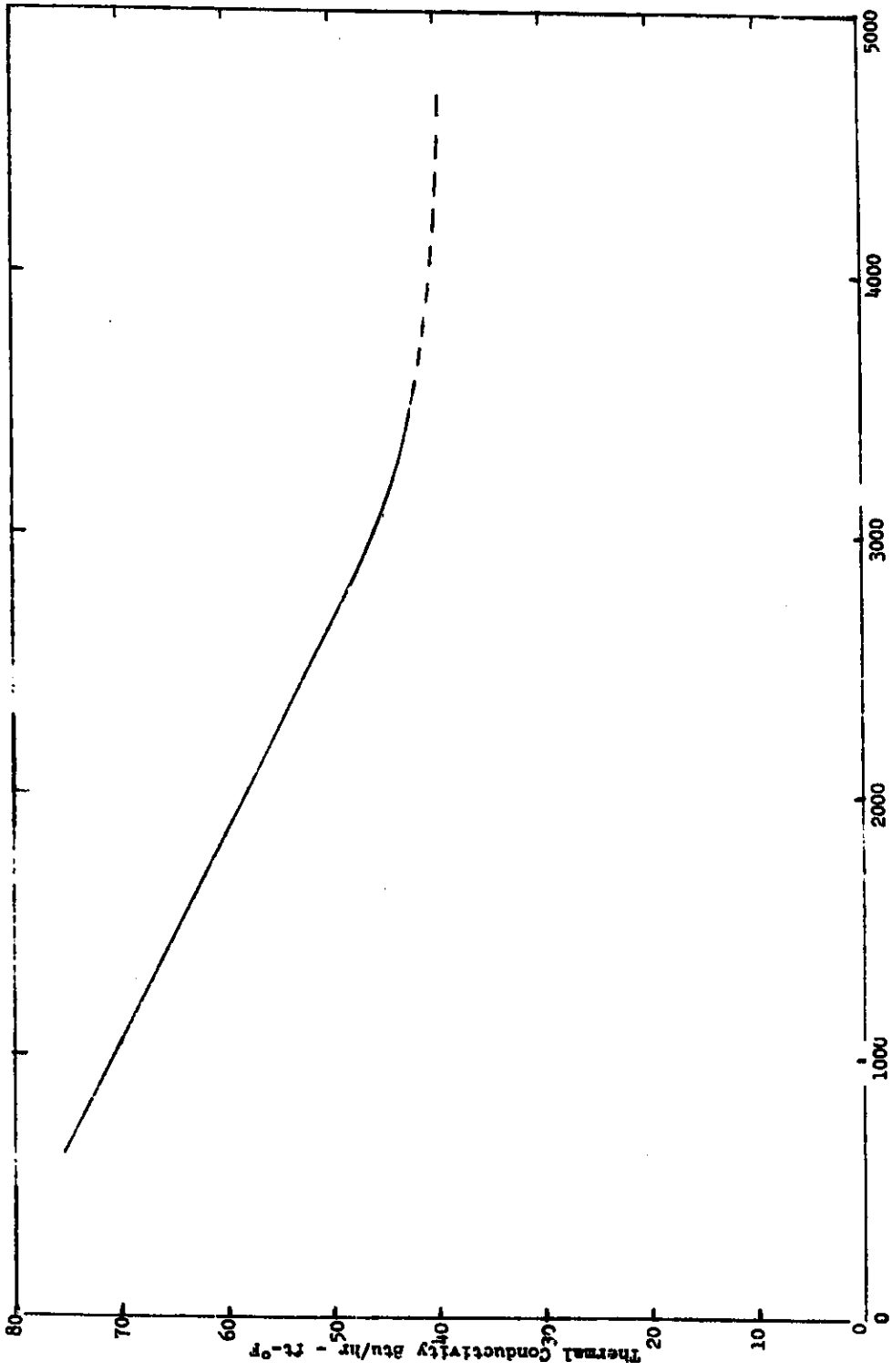

FIGURE B-3 Thermal Conductivity of Molybdenum

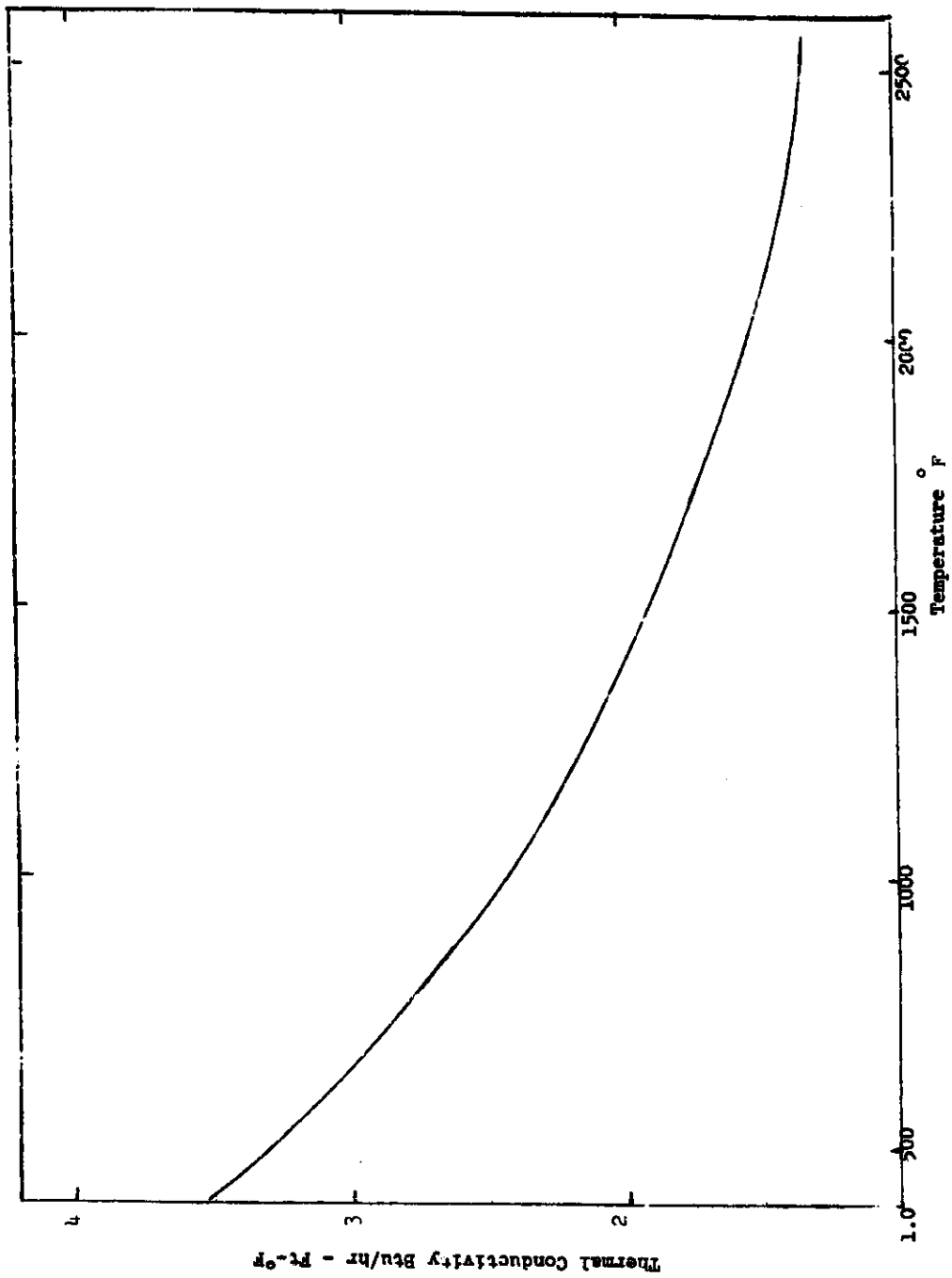

FIGURE B-4 Thermal Conductivity of UO_2

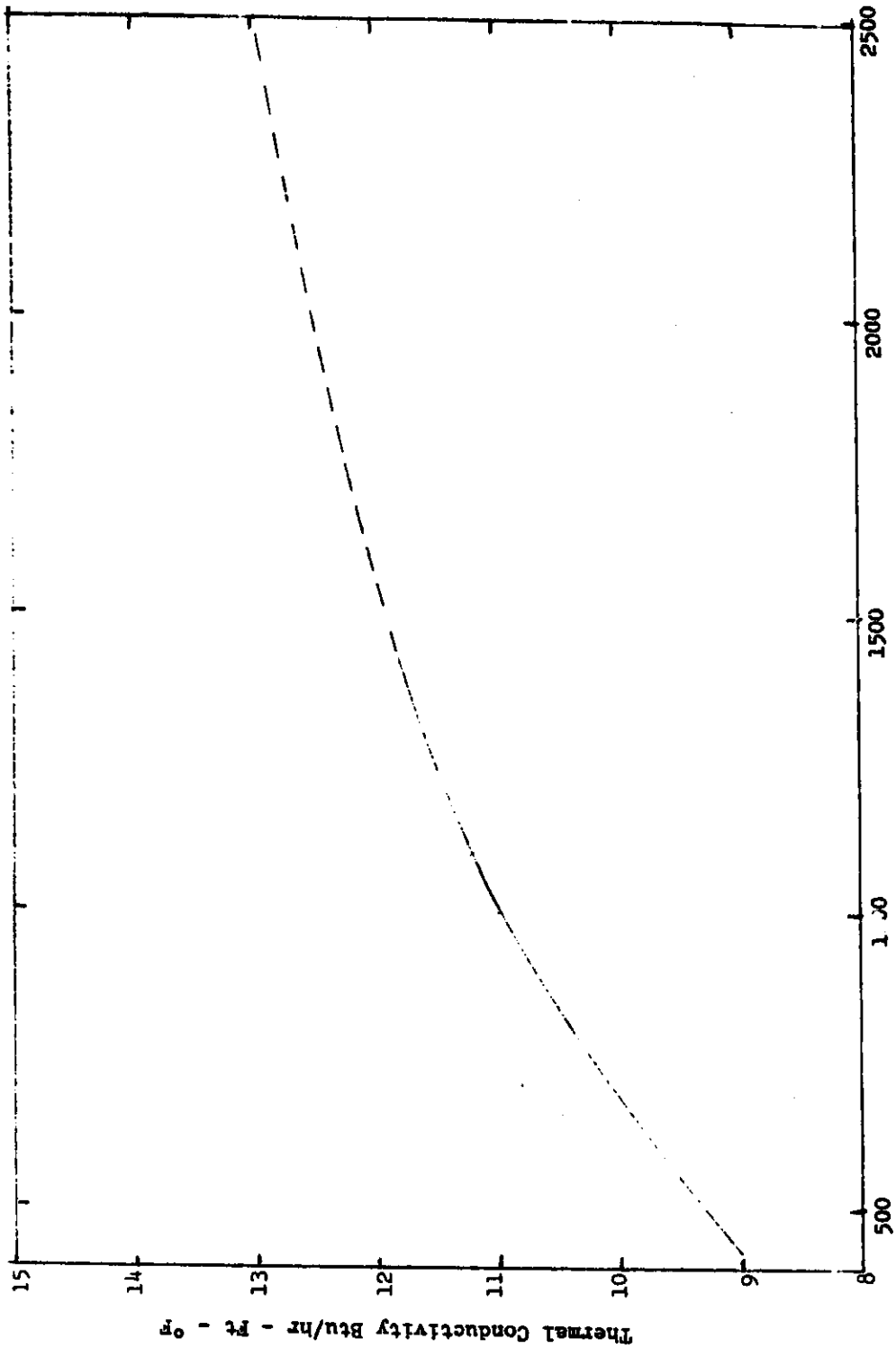

FIGURE B-5 Thermal Conductivity of PuN

APPENDIX C

GEOMETRIC PARAMETERS

C-1 CORE MODEL DESCRIPTIONS

Two hexagon models, internally-cooled and fuel pin models, were reduced to right circular cylinders to simplify the neutronic, hydraulic, and heat transfer investigation. The neutronic model, referred to as the physics model in Figure C-1 contains the same tube, and fuel arrangement as the hexagon cores. Equivalent areas were devoted to the core components and thus the cross-section area remained the same.

However, the heat transfer model eliminated portions of the core not pertinent to the hydraulic and heat removal considerations. Areas eliminated were those occupied by:

- Subassembly support cladding
- Thermal spacing between subassemblies
- Void space within the cermet fuel

Both the physics and heat transfer models contained the following components in equal quantities:

- 100% theoretical dense cermet
- Tube cladding
- Coolant

Figures C-1, C-2 and C-3 show the models and the two fuel geometries investigated in the study.

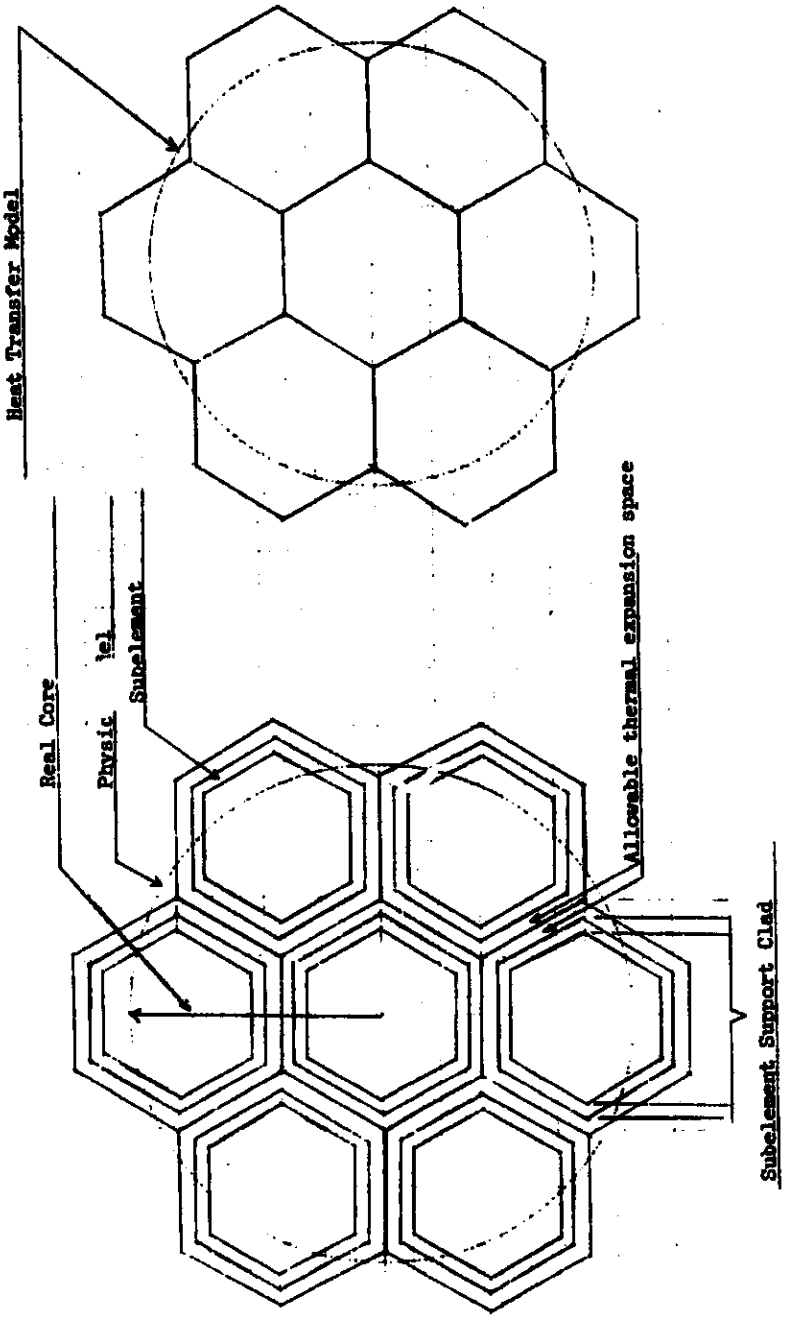

FIGURE C-1 Core Model Representations

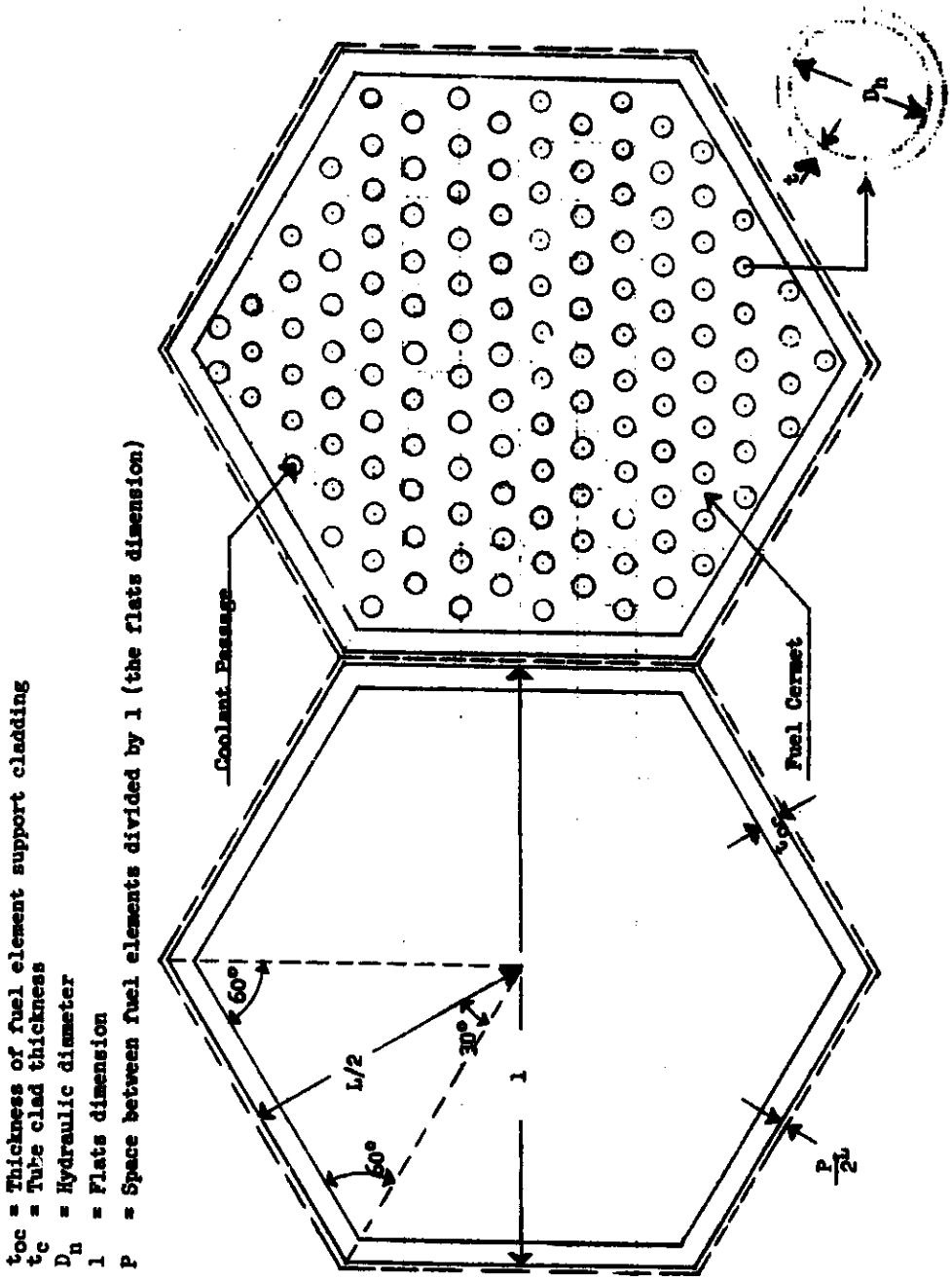

t_{oc} = Thickness of fuel element support cladding
t_c = Tube clad thickness
D_n = Hydraulic diameter
l = Flats dimension
P = Space between fuel elements divided by 1 (the flats dimension)

FIGURE C-2 Internally-Cooled Fuel Element

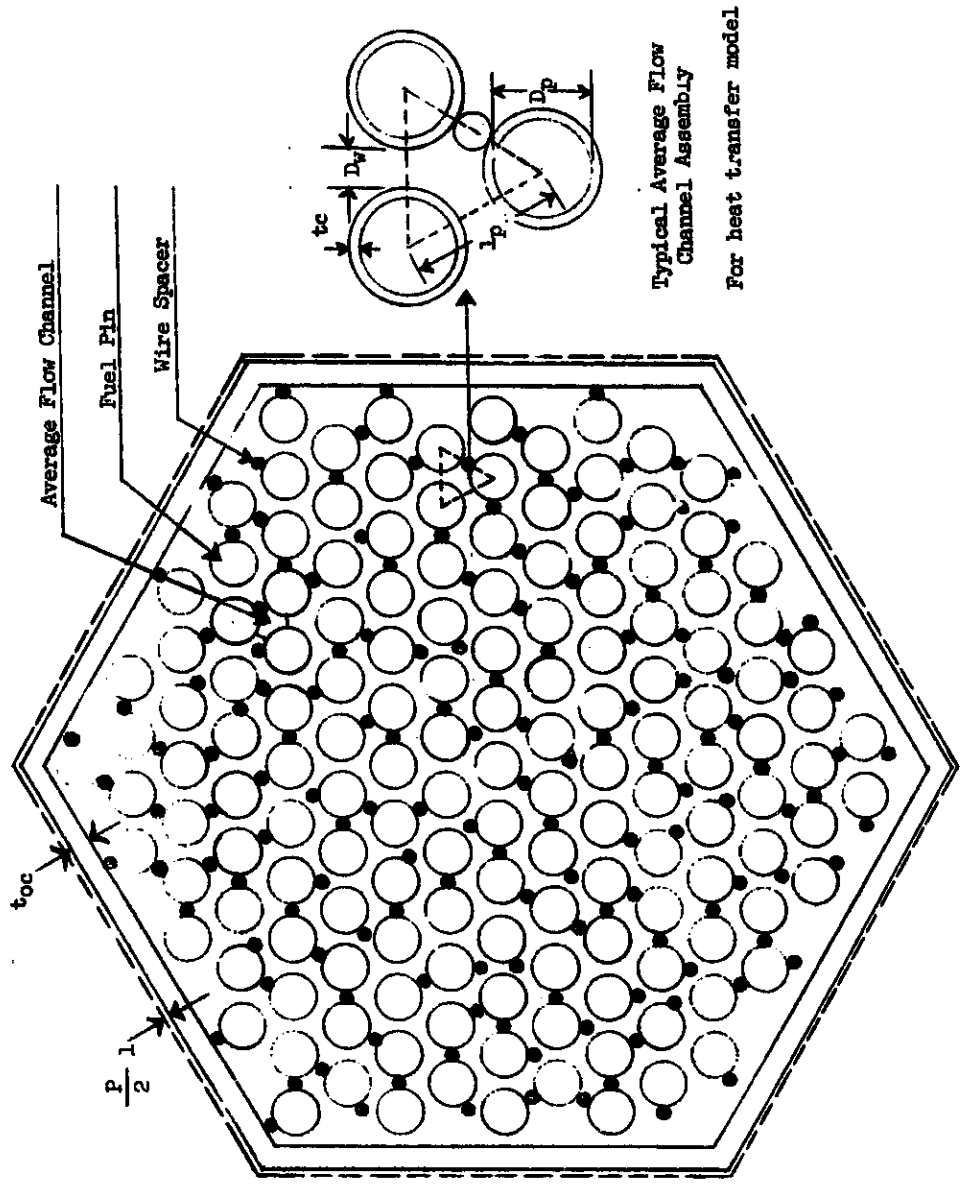

FIGURE C-3 Pin Subassembly Model

Elimination of the above specified areas necessitated re-evaluation and normalization of the (cermet fraction) to a value appropriate to the heat transfer model. The importance of this parameter results from its usage as an index relating parameters for data interpretation. It is defined to be the core fraction occupied by 100% theoretical dense cermet fuel. To differentiate values between the two cores, a prime is used to designate the normalized heat transfer quantity thus, $(\text{cermet fraction})'$ or $(1\text{-cermet fraction})'$.

C.2 INTERNALLY-COOLED CORE MODEL

A detailed geometric description of the internally-cooled core model is given in BNWL-147.[2] The fuel elements are defined in this study as hexagonal shaped subelements and consist of finely divided fissile material embedded in a continuous molybdenum matrix. Circular coolant passages are arranged in equilateral triangular array throughout the fuel as illustrated in Figure C-2. The necessity of adapting the computer code to include investigation of pin core resulted in the development of equations defining the heat transfer model radius and void fraction independent of geometry. The equations facilitate computer calculations reducing input work requirements. Therefore, a less detailed, but sufficient, analytical model description will be included.

Figure C-2 shows typical elements of an internally-cooled core. A single fuel element is selected to simplify calculations since it is representative of the entire core. The element consists of cermet,

cermet voids, tube clad, coolant, fuel element support clad, and space between fuel elements. The cross-sectional areas per fuel element thus occupied can be calculated as follows:

The area of the fuel element excluding space between elements is A_b. A_b is a function of the triangular segment shown in Figure C-2 and can be expressed as:

$$A_b = 6(1/2 \text{ base x height})$$

where

$$\text{base} = \frac{\ell/2}{\text{Cos}30} = \frac{\ell}{2\text{Cos}30}$$

$$\text{height} = \ell/2$$

Substituting these values into the above equation gives:

$$A_b = 3\left(\frac{\ell}{2\text{Cos}30}\right)\frac{\ell}{2} = \frac{3\ell^2}{4\text{Cos}30}$$

$$A_b = .866\ \ell^2 \qquad \text{(I-1)}$$

Now, define A_{oc} to be the cross-sectional area containing fuel element support clad and

$$t_{oc} = f_1(\ell/2)$$

where

f_1 is some equality constant

$A_{oc} = A_b - 6(1/2 \text{ base x height})$

[redacted]

where

$$\text{height} = \ell/2 - t_{oc} = \ell/2\,(1 - f_1)$$

$$\text{base} = \frac{\ell/2\,(1 - f_1)}{\cos 30^\circ} \quad \frac{\ell(1 - f_1)}{2\,(.866)}$$

$$A_{oc} = .866\,\ell^2 - 3\left[\ell/2\,\frac{(1 - f_1)}{.866}\right]\left[\ell/2\,(1 - f_1)\right]$$

$$A_{oc} = .866\,\ell^2 - \frac{3}{4\,(.866)}\,\ell^2\,(1 - f_1)^2$$

$$A_{oc} = .866\,\ell^2 - .866\,\ell^2\,(1 - f_1)^2$$

$$A_{oc} = .866\,\ell^2\left[1 - (1 - f_1)^2\right]$$

$$A_{oc} = .866\,\ell^2\left[1 - (1 - f_1)^2\right] \qquad \text{(I-2)}$$

Area taken by space between fuel elements becomes:

$$A_s = 6\,[1/2\ \text{base} \times \text{height}] - A_b$$

where the base and height are now defined by:

$$\text{base} = \left(\frac{1 + P}{\cos 30}\right)\ \ell/2 = \left(\frac{1 + P}{.866}\right)\ \ell/2$$

$$\text{height} = (1 + P)\ \ell/2$$

$$A_s = 6/2 \left[\left(\frac{1 + P}{.866}\right) \ell/2 \; (1 + P) \; \ell/2\right] - .866 \; \ell^2$$

$$A_s = \left[3/4 \left(\frac{1 + P}{.866}\right)^2 - .866\right] \ell^2$$

$$A_s = .866 \; \ell^2 \left[(1 + P)^2 - 1\right] \qquad \text{(I-3)}$$

The physics model is based on a right circular cylinder with a total core area of A_p.

$$A_p = (A_s + A_o) \; N_b$$

where

N_b = the number of fuel elements per core.

Thus,

$$A_p = .866 \; N_b \ell^2 \left[(1 + P)^2 - 1 + 1\right]$$

$$A_p = .866 \; \ell^2 N_b \; (1 + P)^2$$

or

$$\pi r_{eq}^{\;2} = .866 \; \ell^2 N_b \; (1 + P)^2 \qquad \text{(I-4)}$$

where

r_{eq} is defined as the equivalent core radius.

The heat transfer model is based on a right circular cylinder but with a core area of:

$$A_h = (A_b - A_{oc} - A_f) N_b = \pi \; r'^{\;2}_{eq} \qquad \text{(9A)}$$

where

A_f = the cross section area occupied by voids in the fuel cermet.

r'_{eq} = the equivalent heat transfer model radius.

The cross-sectional area of a fuel element taken by coolant = A_c

$$A_c = \frac{\pi D_h^2 N_t}{4} \qquad \text{(I-5)}$$

where

N_t = the number of coolant tubes per fuel element.

Let A_{tc} represent the area occupied by the coolant tube clad. Then, from Figure A-2

$$A_{tc} = \frac{\pi(D_o^2 - D_h^2)N_t}{4}$$

where

$$D_o = (D_h + 2tc)$$

$$A_{tc} = \pi/4\ [(D_h + 2tc)^2 - D_h^2]N_t$$

$$A_{tc} = \pi tc\ (D_h + tc)N_t \qquad \text{(I-6)}$$

The area occupied by 100% theoretical density fuel is A_F. Defining α_p to be the value (1-cermet fraction), the following relationship is valid.

$$A_F = (1 - \alpha_p)\ (A_p + A_s)$$

$$A_F = (1 - \alpha_p)\ [.866\ \ell^2\ (1 + P)^2] \qquad \text{(I-7)}$$

Now define ρ to be the fuel density and ρ_t the 100% theoretical density. The area of the fuel void is:

$$\rho/\rho_t \ (A_F + A_f) = A_F$$

$$A_f = (\frac{\rho_t}{\rho} - 1)A_F$$

or, substitution for A_F gives:

$$A_f = (\rho_t/\rho - 1)\ (1 - \alpha_r)\ [.866\ \ell^2\ (1 + P)^2] \qquad \text{(I-8)}$$

And, finally, the heat transfer model area becomes:

$$A_h = N_b\ [.866\ \ell^2 - .866\ \ell^2\ [1 - (1-f_1)^2] - (\rho_t/\rho-1)(1-\alpha_p)$$

$$[.866\ \ell^2\ (1+P)^2]]$$

or

$$\pi\ r'^2_{eq} = .866\ \ell^2\ N_b\ [(1-f_1)^2 - (\rho_t/\rho\ - 1)(1-\alpha_p)(1+P)^2] \qquad \text{(I-9)}$$

The core component fractions can now be calculated:

$$\alpha_{oc} = \frac{N_b A_{oc}}{A_p} = \frac{N_b\ .866\ \ell^2\ [1-(1-f_1)^2]}{N_b\ .866\ \ell^2\ (1+P)^2}$$

$$\alpha_{cc} = \frac{1-(1-f_1)^2}{(1+P)^2} \qquad \text{(I-10)}$$

$$\alpha_s = \frac{N_b A_s}{A_F} = \frac{N_b \cdot .866\ \ell^2\ [(1+P)^2 - 1]}{N_b \cdot .866\ \ell^2\ (1+P)^2}$$

$$\alpha_s = \frac{(1+P)^2 - 1}{(1+P)^2} \qquad \text{(I-11)}$$

$$\alpha_c = \frac{N_b A_c}{A_p} = \frac{\pi D_h^{\,2} N_c}{4\ (\pi r_{eq}^{\,2})}$$

$$\alpha_c = \frac{D_h^{\,2} N_c}{4\ r_{eq}^{\,2}} \qquad \text{(I-12)}$$

$$\alpha_{tc} = \frac{A_{tc}}{A_p} = \frac{\pi tc\ (D_h + {}_{tc})\ N_c}{\pi r_{eq}^{\,2}}$$

$$\alpha_{tc} = \frac{tc\ (D_h + {}_{tc})\ N_c}{r_{eq}^{\,2}} \qquad \text{(I-13)}$$

$$\alpha_f = \frac{A_f}{A_p} = \frac{N_b \cdot .866\ \ell^2\ [(\rho_t/\rho - 1)\ (1-\alpha_p)\ (1+P)^2]}{N_b \cdot .866\ \ell^2\ (1+P)^2}$$

$$\alpha_f = (\rho_t/\rho - 1)\ (1-\alpha_p) \qquad \text{(I-14)}$$

$$\alpha_F = (1-\alpha_p) \qquad \text{(I-15)}$$

where

α_{oc} = the void fraction occupied by fuel element support clad

α_s = the void fraction occupied by space between fuel elements

α_c = void fraction occupied by coolant

α_{tc} = void fraction occupied by tube clad

α_f = void fraction occupied by space within the cermet

α_F = the void fraction occupied by 100% theoretical density cermet

$$\alpha_p = \alpha_s + \alpha_{oc} + \alpha_c + \alpha_{tc} + \alpha_f$$

The heat transfer model equivalent radius can now be evaluated. Dividing Equation (9) by (4) gives a relationship between the two radii:

$$\frac{\pi r'^2_{eq}}{\pi r^2_{eq}} = \frac{.866\ \ell^2 N_b \left[(1-f_1)^2 - (\rho_t/\rho - 1)\ (1-\alpha_p)\ (1+P)^2\right]}{.866\ \ell^2 N_b\ (1+P)^2}$$

$$\frac{r'^2_{eq}}{r^2_{eq}} = \frac{(1-f_1)^2 - (\rho_t/\rho - 1)\ (1-\alpha_p)\ (1+P)^2}{(1+P)^2}$$

$$\frac{r'^2_{eq}}{r^2_{eq}} = \frac{(1-f_1)^2}{(1+P)^2} - (\rho_t/\rho - 1)\ (1-\alpha_p)$$

But

$$\frac{(1-f_1)^2}{(1+P)^2} = \frac{1}{(1+P)^2} - \alpha_{oc}$$ From Eq. I-10

$$\frac{1}{(1+P)^2} =, 1 - \alpha_s$$ From Eq. I-11

[redacted] DECLASSIFIED

$$\left(\frac{\rho t}{\rho} - 1\right)(1 - \alpha_p) = \alpha_f$$

From Eq. I-14

Therefore substitution gives:

$$\frac{r'^{2}_{eq}}{r'^{2}_{eq}} = 1 - \alpha_s - \alpha_{oc} - \alpha_f \qquad \text{(I-16)}$$

and the heat transfer model equivalent radius is:

$$r'_{eq} = r_{eq}\sqrt{1 - \alpha_s - \alpha_{oc} - \alpha_f} \qquad \text{(I-17)}$$

Note that the expression r'_{eq} is independent of geometry and therefore is valid for both the internally-cooled and pin core.

The necessary condition for the value (1-cermet fraction)' for the heat transfer model is:

$$(1 - \alpha_p)\,\pi r_{eq}^{2} = (1 - \alpha'_h)\,\pi r'^{2}_{eq} \qquad \text{(I-18)}$$

This expression requires the same quantity of cermet to exist in both cores. Divising through by $(1 - \alpha'_h)$ and r_{eq}^{2} gives:

$$\frac{r'^{2}_{eq}}{r'^{2}_{eq}} = \frac{1 - \alpha_p}{1 - \alpha'_h} \qquad \text{(I-19)}$$

[redacted]

Replacing the radius ratio with its equivalent from Equation I-16:

$$\frac{r'^{2}_{eq}}{r^{2}_{eq}} = 1 - \alpha_s - \alpha_{oc} - \alpha_f \qquad \text{(I-16)}$$

finally defines α'_h as:

$$\alpha'_h = 1 - \left(\frac{1 - \alpha_p}{1 - \alpha_s - \alpha_{oc} - \alpha_f}\right) \qquad \text{(I-20)}$$

This equation relates the internally-cooled and pin model such that the same input data is utilized for both cores. However, modification for α'_{oc} in the pin model is necessary, as will be indicated in that section.

C.3 PIN CORE

This model consists of hexagonal subassemblies containing fuel pins in equilateral triangular array with pin spacing maintained by wire wrapping about each pin. Figure C-3 shows a typical subassembly indicating the similarity to the internally-cooled fuel element of Figure C-2. The major differences are changes in fuel and coolant location within the core, and for the pin model, addition of wire wrap, and a substantial increase in the flat dimension. Assumptions made were:

(1) Pin spacer is 1-columbium 0.1-zirconium-alloy wire with 6 wraps per foot.

(2) The hydraulic diameter is the same for both cores.

(3) Other input data is to be the same.

(4) An average of one wire spacer per pin exists in the cross section.

(5) The geometric arrangement is such that an average number of fuel pins and wire spacers per coolant channel is 1 to 2. This assumption pertains to the void and area considerations only.

(6) The pin core subassembly can be larger than the internally-cooled ful element with nineteen subassemblies per core as reasonable.

(7) The wire spacers contribute to heat transfer considerations and are included in the heat transfer model (1-cermet fraction)

(8) The tube claddin- can be considered as part of the fuel for maximum fuel temperature calculations. This appears conservative since the clad thermal conductivity is higher than the cermet.

The development of equations relating the two cores can be as follows. The heat transfer pin model containing coolant, tube clad wire spacer and cermet (excluding subassembly support clad, spacing between subassemblies and area of fuel voids) is defined in the core cross section by:

$$(A_c + A_{tc} + A_w)\, N_b = \alpha'_h\, \pi r'^2_{eq} \qquad \text{(P-1)}$$

[redacted]

where

A_c = coolant area per subassembly

A_{tc} = tube clad area per subassembly

A_w = wire spacer area per subassembly

N_b = total number of subassemblies per core

α'_h = the total void fraction in the heat transfer core model

r'_{eq} = equivalent heat transfer model radius.

Rearrangement of the hydraulic diameter equation gives the following relationship:

$$N_b A_c = \frac{N_t D_h C N_b}{4} \qquad \text{(P-2)}$$

where

N_t = total coolant passages per subassembly

D_h = the hydraulic diameter

C = the wetted perimeter per coolant passage

$N_t N_b = N_c$ the total coolant passages per core.

Now define

D_p = inside pin diameter

D_w = wire diameter

l_p = distance between pins

P_p = outside pin perimeter

Then from Figure C-3 the following expressions are obtained.

$$D_w = l_p - (D_p + 2tc)$$

$$P_p = \pi (D_p + 2tc)$$

also

$$P_p = 2C - \pi D_w$$

Equating the two pin perimeter equations and solving for the pin diameter:

$$D_p = \frac{2C - \pi D_w}{\pi} - 2tc$$

$$D_p = \frac{2C}{\pi} - D_w - 2tc \qquad \text{(P-3)}$$

or

$$D_w = \frac{2C}{\pi} - D_p - 2tc \qquad \text{(P-4)}$$

Comparison of Equation 4 with the initial equation defining D_w indicates the following relationship for l_p

$$l_p = \frac{2C}{\pi} \qquad \text{(P-5)}$$

Equations P-3 and P-4 are not independent and hence, there exist 6 unknowns, namely (N_t, N_b, C, D_p and D_w), and only 4 equations (Eq. 1, 2, 3 or 4, and 5). Development of other equations may proceed as follows.

The total heat transfer model area is:

$$A_h = \pi r'^2_{eq}$$

[redacted]

From Figure C-3 the following is also true:

$$A_h = 1/2\ l_p\ (l_p \cos 30)\ N_c$$

$$A_h = N_c \frac{l_p^2 \cos 30}{2}$$

where

$N_c = N_t\ N_b$ (the total number of coolant passages).

but Equation 5 defines:

$$l_p = \frac{2C}{\pi}$$

equating the two expressions defining A_h and substitution for l_p gives:

$$\pi r'^2_{eq} = \frac{2\ N_c\ C^2 \cos 30}{\pi^2}$$

solving for the total number of coolant passages per core:

$$N_c = \frac{\pi 3\ r'^2_{eq}}{2\ C^2 \cos 30} \qquad \text{(P-6)}$$

The total cross section area equations for the tube clad, wire spacer and fuel can be calculated from Figure C-3 also. These relationships are:

$$N_b\ A_{tc} = \frac{N_c \pi}{2}\ (D_p\ tc + tc^2) \qquad \text{(P-7)}$$

and

$$N_b\ A_w = \frac{N_c \pi}{8}\ D_w^2 \qquad \text{(P-8)}$$

[redacted]

Two other conditions are:

$$N_b A_F = \left(\frac{\pi D_p^2}{4}\right) \frac{N_c}{2}$$

$$N_b A_F = (1 - \alpha'_h)\, \pi r'^2_{eq}$$

thus

$$\frac{N_c D_p^2}{8} = (1 - \alpha'_h)\, r'^2_{eq} \qquad \text{(P-9)}$$

A summary of equations to be used are:

$$(A_c + A_{tc} + A_w)\, N_b = \alpha'_h\, \pi r'^2_{eq} \qquad \text{(P-1)}$$

$$N_b A_c = \frac{N_c C D_h}{4} \qquad \text{(P-2)}$$

$$D_p = \frac{2C}{\pi} - D_w - 2tc \qquad \text{(P-3)}$$

$$N_c = \frac{\pi 3\, r'^2_{eq}}{2C^2 \cos 30} \qquad \text{(P-6)}$$

$$N_b A_{tc} = \frac{N_c \pi}{2}\, tc\, (D_p + tc) \qquad \text{(P-7)}$$

$$N_b A_w = \frac{N_c \pi}{8} D_w^2 \qquad \text{(P-8)}$$

$$\left(\frac{D_p^2}{8}\right) N_c = (1 - \alpha'_h)\, r'^2_{eq} \qquad \text{(P-9)}$$

Thus 7 equations define 7 unknowns. The unknowns are $(N_b A_c)$, $(N_b A_{tc})$, $(N_b A_w)$, D_p, C, N_c, and D_w. A process of "unknown elimination" from these equations result in an expression for the wetted perimeter (C).

[redacted]

First eliminating the total coolant passages (N_c) gives:

$$N_c = \frac{4N_b A_c}{C D_h}$$ From Eq. P-2

$$N_c = \frac{\pi 3 r'^2_{eq}}{2C^2 \cos 30}$$ From Eq. P-6

$$N_c = \frac{2N_b A_{tc}}{\pi tc (D_p + tc)}$$ From Eq. P-7

$$N_c = \frac{8 N_b A_w}{\pi D_w^2}$$ From Eq. P-8

$$N_c = \frac{8 (1 - \alpha'_h) r'^2_{eq}}{D_p^2}$$ From Eq. P-9

The 6 reduced equations are:

$$(A_c + A_{tc} + A_w) N_b = \pi \alpha'_h r'^2_{eq}$$ (P-1)

$$D_w = \frac{2C}{\pi} - D_p - 2_{tc}$$ (P-3)

$$N_b A_c = \frac{\pi 3 D_h r'^2_{eq}}{8 C \cos 30}$$ (P-10) (From P-2, 6)

$$N_b A_{tc} = \frac{\pi 4 tc (D_p + tc) r'^2_{eq}}{4 C^2 \cos 30}$$ (P-11) (From P-6, 7)

$$D_w = \frac{D_p}{r'_{eq}} \sqrt{\frac{N_b A_w}{\pi (1 - \alpha'_h)}}$$ (P-12) (From P-8, 9)

$$D_p = 4\,C\sqrt{\frac{(1-\alpha'_h)\cos 30}{\pi^3}}$$

(P-13) (From P-6, 9)

Next the wire diameter (D_w) is eliminated by equating equations 3 and 12. The resulting reduced equations are:

$$(A_c + A_{tc} + A_w)\,N_b = \pi\alpha'_h\,r'^2_{eq} \qquad \text{(P-1)}$$

$$N_b A_c = \frac{\pi^3 D_h\,r'^2_{eq}}{8C\cos 30} \qquad \text{(P-10)}$$

$$N_b A_{tc} = \frac{\pi^4 tc\,(D_p+tc)\,r'^2_{eq}}{4C^2\cos 30} \qquad \text{(P-11)}$$

$$N_b A_w = \frac{\pi r'^2_{eq}\,(1-\alpha'_h)\,(\frac{2C}{\pi} - D_p - 2tc)^2}{D_p^2} \qquad \text{(P-12)}$$

$$D_p = 4\,C\sqrt{\frac{(1-\alpha'_h)\cos 30}{\pi^3}} \qquad \text{(P-13)}$$

Substitution of equations P-10, 11 and 14 into P-1 results in an expression for the total areas $N_b A_c$, $N_b A_{tc}$, and $N_b A_w$ as a function of the pin diameter and wetted perimeter.

The two reduced equations are

$$D_p = 4\,C\sqrt{\frac{(1-\alpha'_h)\cos 30}{\pi^3}}$$

(P-13)

$$D_h + \frac{2\pi tc\,(D_p + tc)}{C} + \frac{8C\cos 30(1-\alpha'_h)\left(\frac{2C}{\pi} - D_p - 2tc\right)^2}{\pi^2 D_p^2} = \frac{8\,\alpha'_h C\cos 30}{\pi^2} \qquad \text{(P-15)}$$

Substitution of Equation P-13 into P-15 and simplifying results in the expression for the wetted perimeter.

$$\left[(2\alpha'_h - 1)\frac{8\cos 30}{\pi^2} - \frac{2}{\pi} + 8\sqrt{\frac{(1-\alpha'_h)\cos 30}{\pi^3}}\right] C^2 +$$

$$\left[4tc - D_h - 16\pi tc\sqrt{\frac{(1-\alpha'_h)\cos 30}{\pi^3}}\right] C - 4\pi tc^2 = 0$$

Now define the following constants

$$X = (2\alpha'_h - 1)\frac{8\cos 30}{\pi^2} - \frac{2}{\pi} + 8\sqrt{\frac{(1-\alpha'_h)\cos 30}{\pi^3}} \qquad \text{(P-16)}$$

$$Y = 4tc - D_h - 16\pi tc\sqrt{\frac{(1-\alpha'_h)\cos 30}{\pi^3}} \qquad \text{(P-17)}$$

$$Z = 4\pi tc^2 \qquad \text{(P-18)}$$

then

$$C = -\frac{Y}{2X} + \sqrt{\left(\frac{Y}{2X}\right)^2 + \frac{Z}{X}} \qquad \text{(P-19)}$$

Thus it is evident that the wetted perimeter is a function of the heat transfer void fraction α'_h. The other parameter values are constant since they are the same for both the internally-cooled and pin core. For complete conversion to the pin core, inspection of α'_h is necessary. The equation is:

$$\alpha'_h = 1 - \left(\frac{1 - \alpha_p}{1 - \alpha_s - \alpha oc - \alpha f}\right)$$

α_p, α_s, and α_f are found to be the same in both cores (compare I-11 and 14 with P-20 and 21). However α_{oc} is dependent on the flats dimension (ℓ) and consequently changes in the pin core since ℓ can be larger for this model (compare I-10 with P-22). The defining equation is:

$$\alpha_{oc} = \frac{1 - (1 - f_2)^2}{(1 + p)^2}$$

where

$$f_2 = \frac{2\ toc}{\ell}$$

Thus α_{oc} is the same for both cores only when $f_1 = f_2$. A method of induction indicated that

$\alpha_{oc} = (\frac{\ell 1}{\ell 2} + .01)\ \alpha_{ocI}$ when ℓ_2 varied within the following limits;

$\ell_p < 4\ell_I$

Error introduced by this expression is negligible. However, modification of the code permitted α_{oc} to be calculated for the pin core with ℓ defined in Equation I-4 and N_b an input item (19 subassemblies per core) completing the code conversion.

Void Fractions

The pin core void fractions were found to be

$$\alpha_s = \frac{(1 + p)^2 - 1}{(1 + p)^2}$$

(P-20 Compare (I-11)

$$\alpha_f = \left(\frac{\rho_t}{\rho} - 1\right)(1 - \alpha_p)$$ (P-21 Compare I-14)

$$\alpha_{oc} = \frac{1 - (1 - f_2)^2}{(1 + p)^2}$$ (P-22 Compare I-10)

$$\alpha_{tc} = \frac{N_c\, tc\, (D_p + tc)}{2r_{eq}^2}$$ (P-24 Compare I-13)

$$\alpha_w = \frac{N_c D_w 2}{8r_{eq}^2}$$ (P-24)

$$\alpha_c = \frac{N_c D_h C}{4\pi r_{eq}^2}$$ (P-25 Compare I-12)

$$\alpha_F = (1 - \alpha_p)$$ (P-26 Compare I-15)

α_F is the same for the internally-cooled core thus requiring the same cermet volume in both models for a given α_p. This requirement tends towards compliance with the criticality curves assumed. However, results indicate a shift to higher void fractions to accommodate similar maximum fuel core temperatures in the pin core.

ACKNOWLEDGMENTS

The contributions of C. E. Leach for his technical assistance is greatly acknowledged. The effort of Billy M. Cole on the preparation of graphs and charts is appreciated.

NOMENCLATURE

A_b = Cross sectional area of core subassembly excluding space between subassemblies.

A_c = Cross sectional area of core subassembly occupied by coolant.

A_F = Cross sectional area of core subassembly occupied by theoretical dense cermet.

A_f = Cross sectional area of core subassembly occupied by fuel voids.

AFL = Total cross sectional area of core occupied by coolant.

A_h = Total core cross sectional area of heat transfer model.

A_{oc} = Cross sectional area of core subassembly occupied by subassembly clad.

A_p = Total core cross sectional area of physics model.

A_s = Cross sectional area of core subassembly occupied by spacing between subassemblies.

A_u = Cross section area of core subassembly occupied by coolant and wire spacers.

A_{tc} = Cross sectional area of core subassembly occupied by fuel pin clad.

A_w = Cross sectional area of core subassembly occupied by wire spacer.

AFU = Total cross sectional area of core occupied by 100% dense cermet.

a = $3Ks/(2Ks+Kp)$

b = Volume fraction of particulate matter.

C = wetted perimeter per coolant passage.

C_u = wetted perimeter calculated excluding wire-spacer surfaces.

ΔP = Pressure drop

ΔP_w = Pressure drop for channels containing wire spacers.

ΔP_n = Pressure drop calculated for a channel containing wire-spacers but excluding the effect of the spacers on pressure drop.

f_1 = $(2toc/\ell)$ the dimensionless subassembly clad thickness for internally-cooled cores.

f_2 = $(2toc/\ell)$ the dimensionless subassembly clad thickness for pin cores.

D_h = Hydraulic diameter.

D_{hu} = Hydraulic diameter calculated for a channel containing wire-spacers but excluding the spacer surfaces from the calculations.

D_o = The outside pin-diameter.

D_p = Fuel diameter

D_w = Spacer wire diameter

G = Mass velocity

G_u = Mass velocity for channels containing wire spacers but including the spacer as part of the coolant.

K_a = Apparent thermal conductivity of a fuel mixture.

K_p = Thermal conductivity of particulate matter (fissile material).

ℓ = Dimension across the flats of the subassembly.

ℓ_I = Flats dimension for internally-cooled cores.

ℓ_p = Pin pitch (center to center spacing between pins)

M = 2.153 times the wire diameter.

N = Ratio of the pressure drop in a channel containing a wire spacer placed parallel to the fuel pin (no wrapping) and ΔP_n.

N_b = Number of fuel subassemblies per core.

N_c = Total number of coolant passages per core.

N_t = Number of coolant passages per subassembly.

n = Number of wire revolutions per unit length of rod.

t_c = Tube clad thickness.

toc = Outer clad thickness of subassembly.

V_{1u} = Inlet velocity without wire spacer.

V_{2u} = Exit velocity without wire spacer.

α_c = Coolant void fraction - physics model.

α_F = Fuel (cermet) fraction - physics model 100% dense

α_f = Fuel void fraction - physics model.

α'_h = Void fraction - heat transfer model.

α_{oc} = Void fraction of subassembly outer clad.

α_p = Total void fraction of physics model.

α_s = Void fraction of space between subassemblies - physics model.

α_{tc} = Void fraction of tube clad - physics model.

ρ = Apparent fuel density

ρ_t = Fuel density at 100% fuel (no voids)

REFERENCES

(1) C. E. Leach, W. W. Little, Jr., L. L. Maas, "Comparison of Plutonium, U^{233}, and U^{235} Fueling for the 710 Reactor," BNWL-117, November 1965.

(2) C. E. Leach, "SWISSCHEESE: A 7090 Fortran IV Code for Thermal-Hydraulic Analysis of Gas-Cooled Nuclear Reactors," BNWL-147. October 1965.

(3) W. W. Little, Jr., and R. W. Hardie, "FCC-A Fundamental Mode Code for Reactor Analysis," BNWL-234 Pacific Northwest Laboratory, Richland Washington, March 1966.

(4) Pratt and Whitney Aircraft Division of United Aircraft Corporation, "LCRE Engineering Report-Design," PWAC-398 Part I Volume I, April 10, 1964.

(5) L. F. Moody, "Friction Factors for Pipe Flow," Trans. ASME, Volume 66, P. 671, 1944.

(6) E. D. Waters, "Effect of Wire Wraps on Pressure Drop for Axial Turbulent Flow Through Rod Bundles," HW-65173 Rev. June 1963.

(7) P. J. Schneider, "Conduction Heat Transfer," Department of Mechanical Engineering University of Minnesota, September 1957.

(8) Pratt and Whitney Aircraft Division of United Aircraft Corporation, "LCRE Engineering Report-Design," PWAC-398 Part I Volume 2, April 10, 1964.

(9) W. D. Weatherford, Jr., John C. Tyler, and P. M. Ku, "Properties of Inorganic Energy-Conversion and Heat Transfer Fluids for Space Applications," Southwest Research Institute, November 1961.

(10) F. J. Tebo, "Selected Values of the Physical Properties of Various Materials," ANL-5914, September 1958.

(11) R. N. Lyon, Editor, "Liquid-Metals Handbook," Second Edition, Washington Atomic Energy Commission, Dept. of the Navy, 1952.

(12) B. W. LeTournear, R. E. Grimble, and J. E. Zerbe, "Pressure Drop for Parallel Flow Through Rod Bundles," Trans. ASME, Vol 79, 1957.

(13) D. A. Dingee and J. W. Chastin, "Heat Transfer From Parallel Rods in Axial Flow," Reactor Heat Transfer Conference of 1956, TID-7529 Part 1 Book 2, 1957.

(14) T. T. Shimazaki and W. J. Freede, "Heat Transfer and Hydraulic Characteristics of the SRE Fuel Element," Reactor Heat Transfer Conference of 1956, TID-7529, Part 1 Book 1, 1957.

(15) A. N. DeStordeur, "Drag Coefficients for Fuel-Element Spacers," Nucleonics. June 1961.

(16) J. C. Maxwell, "On the Motions and Collisions of Perfectly Elastic Spheres," Philosophical Magazine, Volume 19 1860.

(17) M. F. Lyons, R. L. Straley, D. H. Coplin, B. Wiedenbaum, and T. J. Pashos, "UO_2 Thermal Conductivity at Elevated Temperatures," ANS Transactions, June 1963, Meeting, Salt Lake City Utah.

(18) W. M. Pardue, V. W. Storhok, R. A. Smith, P. H. Bonnel, J. E. Gates, and D. L. Keller, "Synthesis Fabrication, and Chemical Reactivity of Plutonium Mononitride," BMI-1693, Battele Memorial Institute, Sept. 1964.

(19) Lockheed Aircraft Corporation - Missiles and Space Division, "Mechanical Oxidation and Thermal Property Data for [Refractory Metals and Their Alloys."